

# DCH performance vs endcap shape and position

Matteo Rama

Giuseppe Finocchiaro

LNF

10 October 2012

# Goals

- Evaluate the DCH performance as a function of the shape and position of the endcaps
  - p resolution
  - K/ $\pi$  separation using dE/dx
  - B $\rightarrow$ D\*K reco. efficiency,  $\Delta E$
- All studies shown in these slides have been produced using FastSim V0.3.2

# Configurations

## common features:

- 10 superlayers, 4 layers each: A A S<sub>+</sub> S<sub>-</sub> S<sub>+</sub> S<sub>-</sub> S<sub>+</sub> S<sub>-</sub> A A
  - |stereo angle|  $\approx 0.06$  rad
  - inner wall radius: 26.5 cm
  - outer wall radius: 80.3 cm
  - sense wires  $r_{\min}$ : 28.6 cm
  - sense wires  $r_{\max}$ : 78.0 cm
- hit spatial resolution: babar-like
- hit efficiency vs polar angle: babar-like (babar-like: tuned on babar data)
- $\sigma(dE/dx)$  modelization: babar-like
  - $\sigma\left(\frac{dE}{dx}\right) = \alpha \left|\frac{dE}{dx}\right|^\beta dx^\gamma$   $\alpha, \beta, \gamma$  tuned on babar data

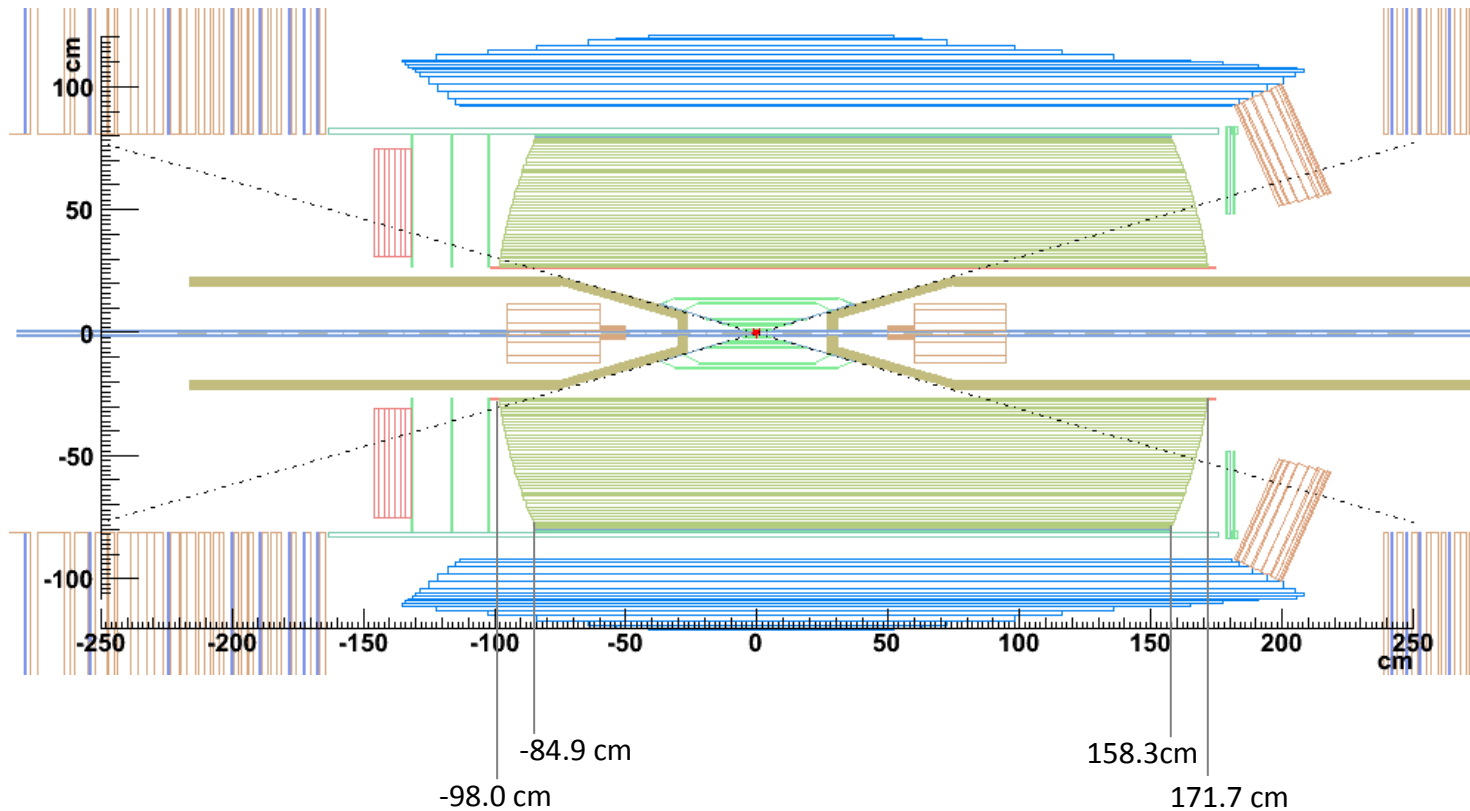
## distinguishing features

- shape and position of endcaps
  - concave/convex
  - varying position along z

**FastSim configurations based on drawings provided by S. Lauciani (see backup slides)**

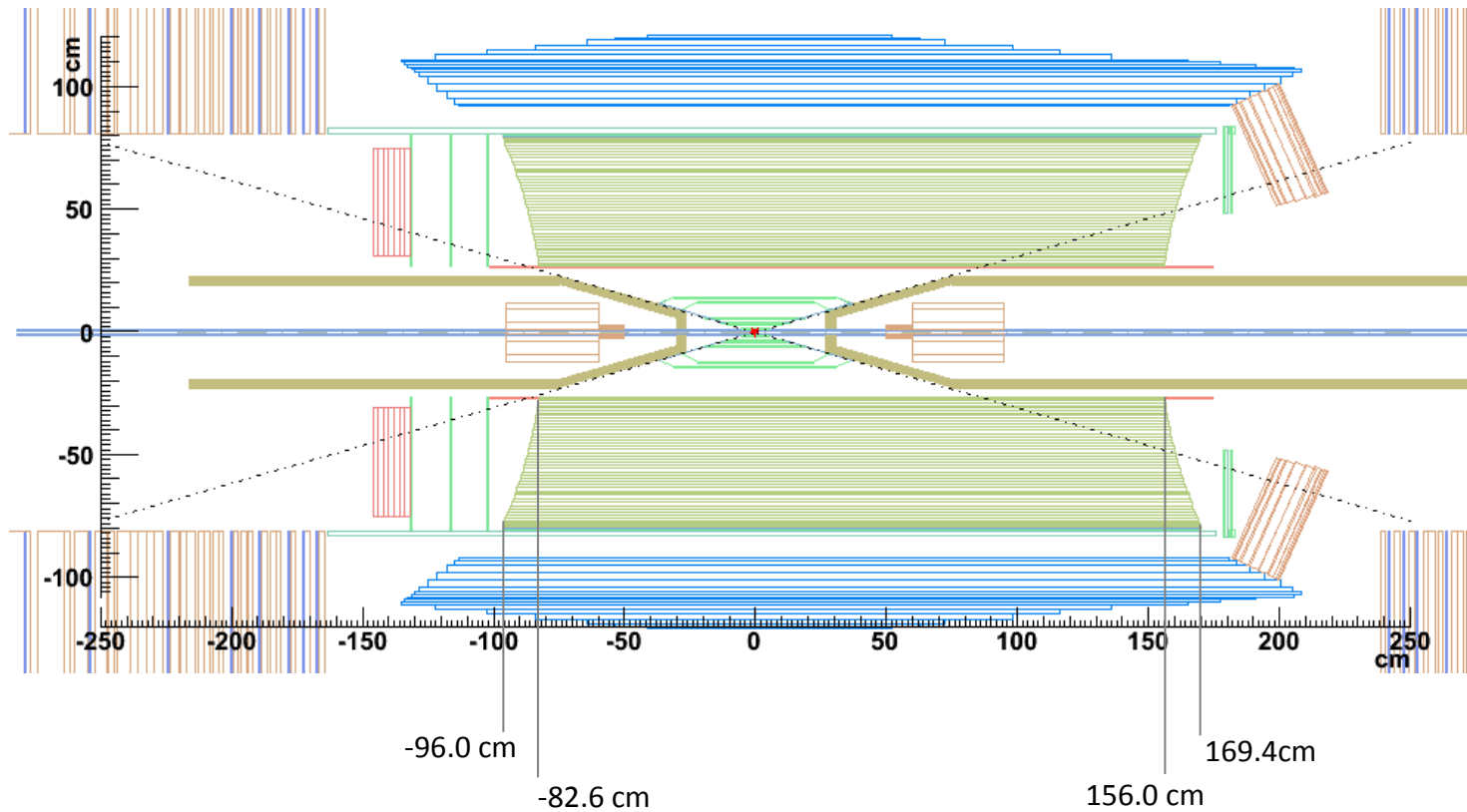
# Option 1

x-z layout in fastsim



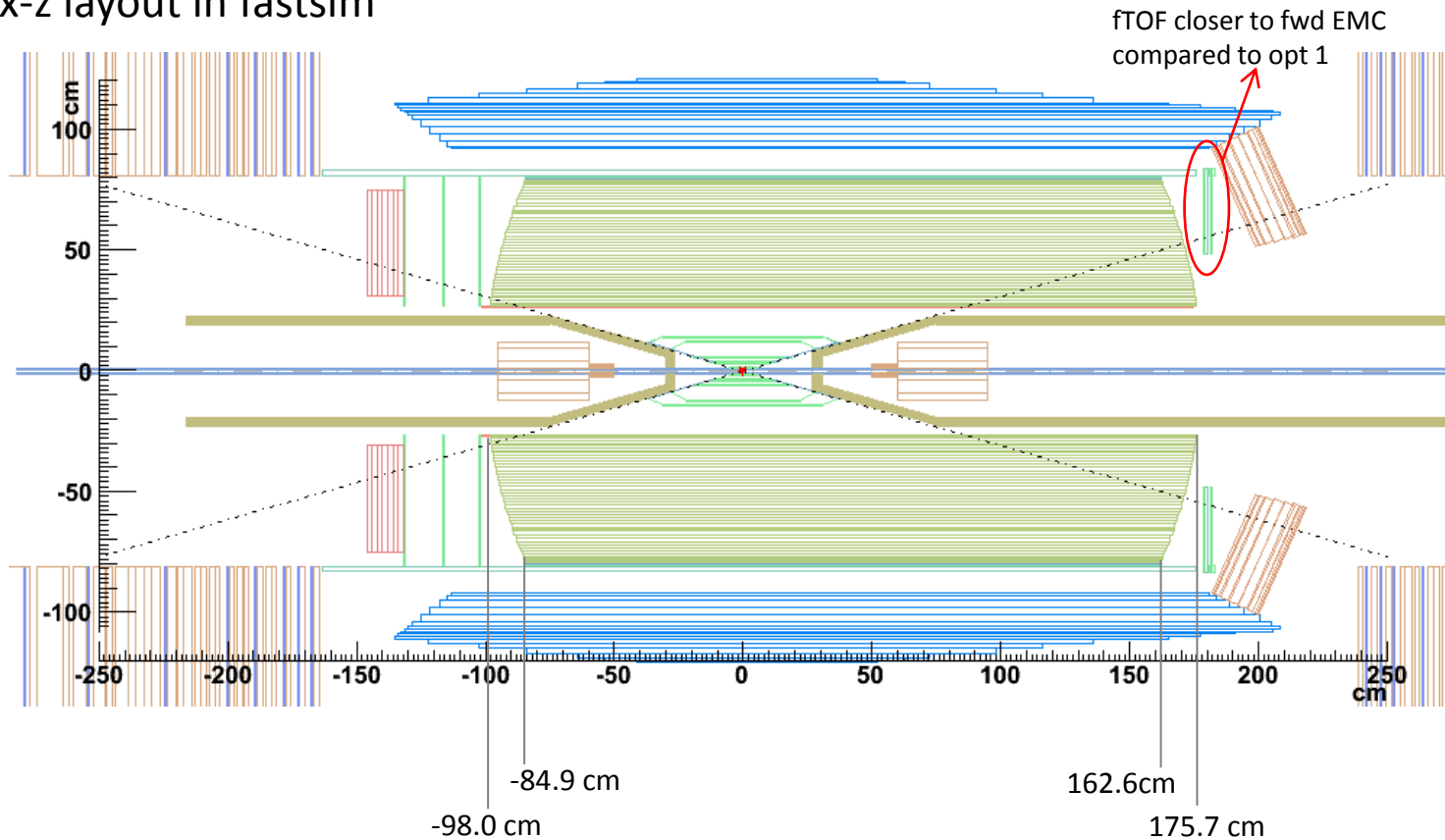
# Option 2

x-z layout in fastsim



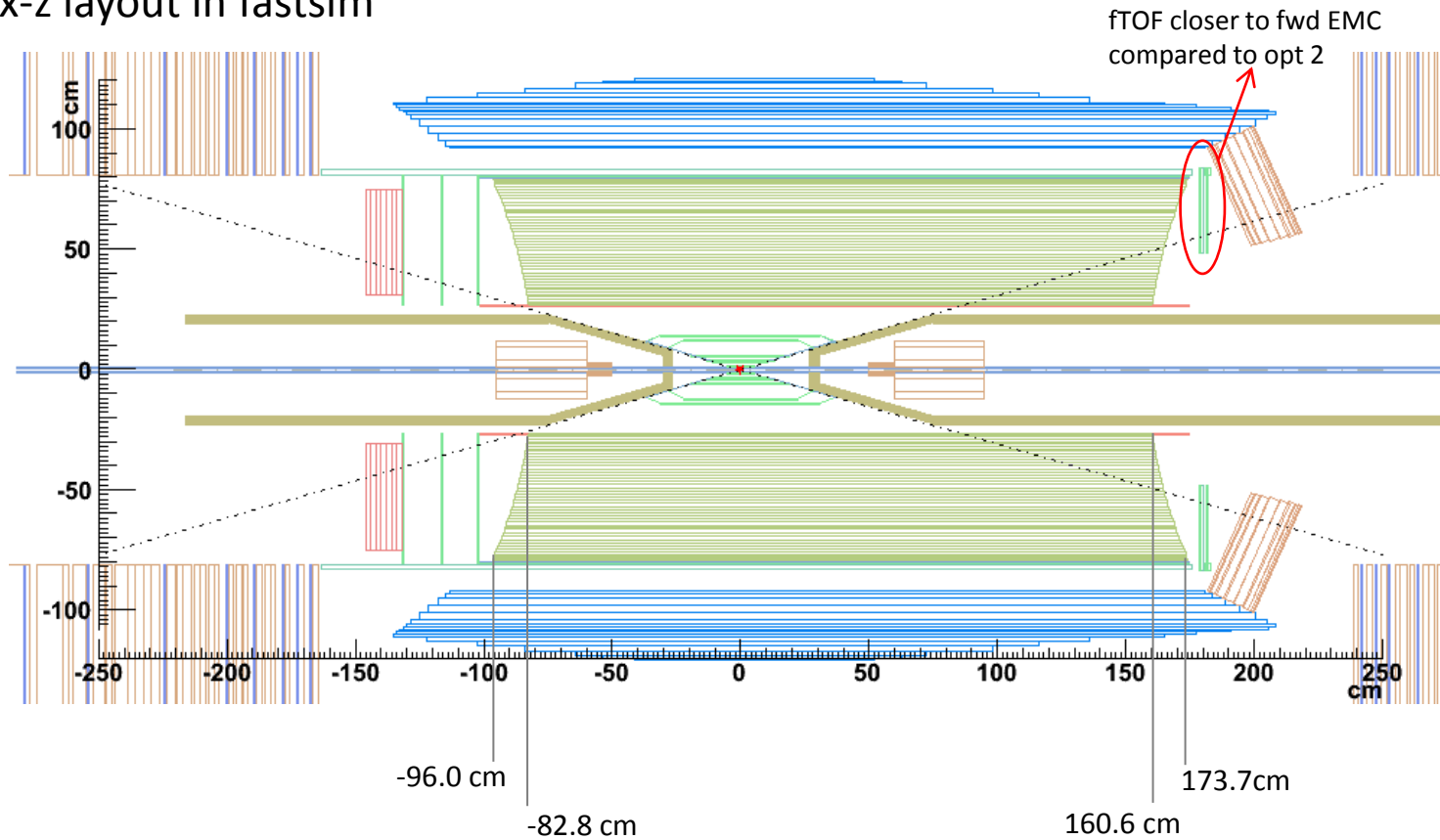
# Option 3

x-z layout in fastsim



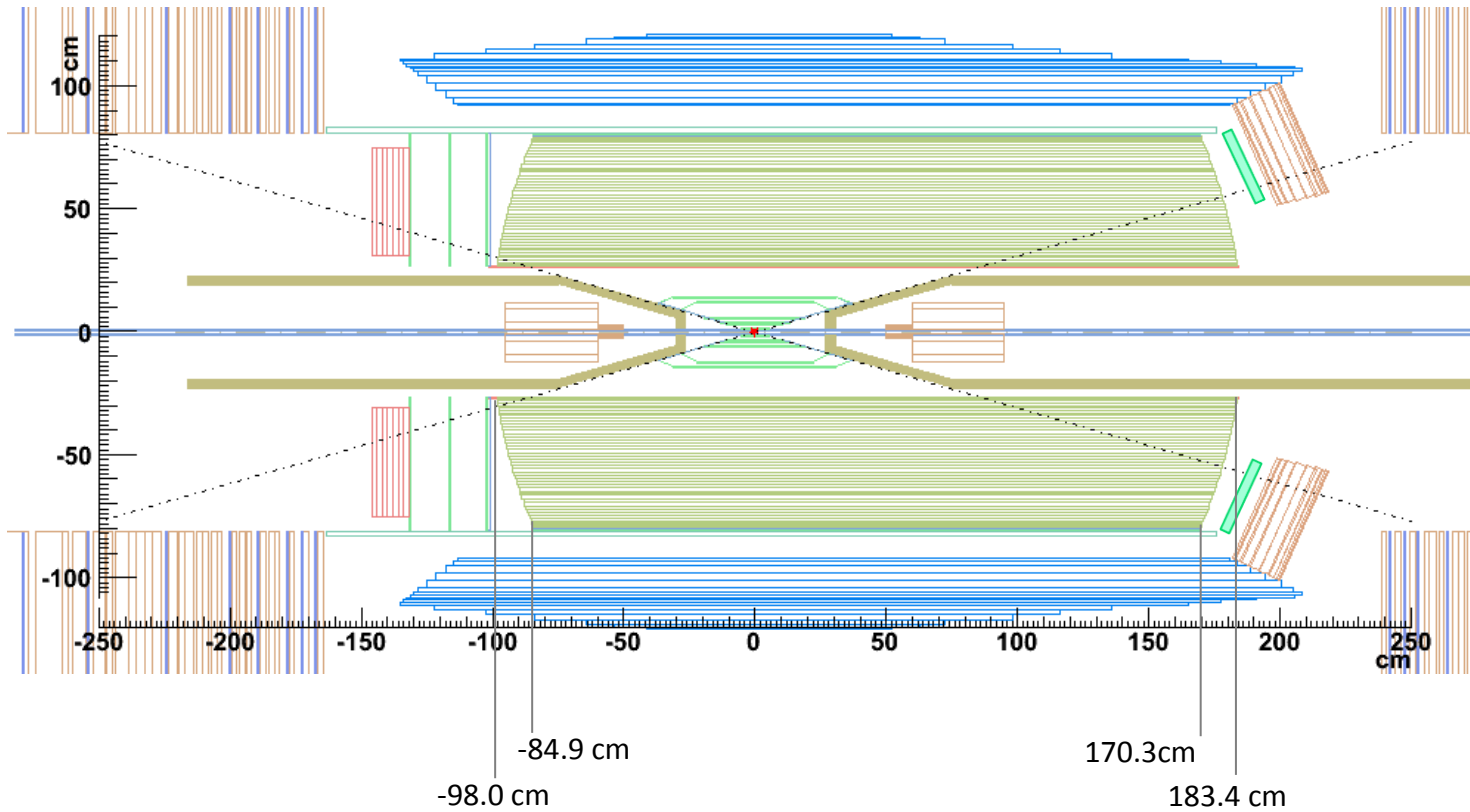
# Option 4

x-z layout in fastsim



# Option 5

x-z layout in fastsim





# Part I

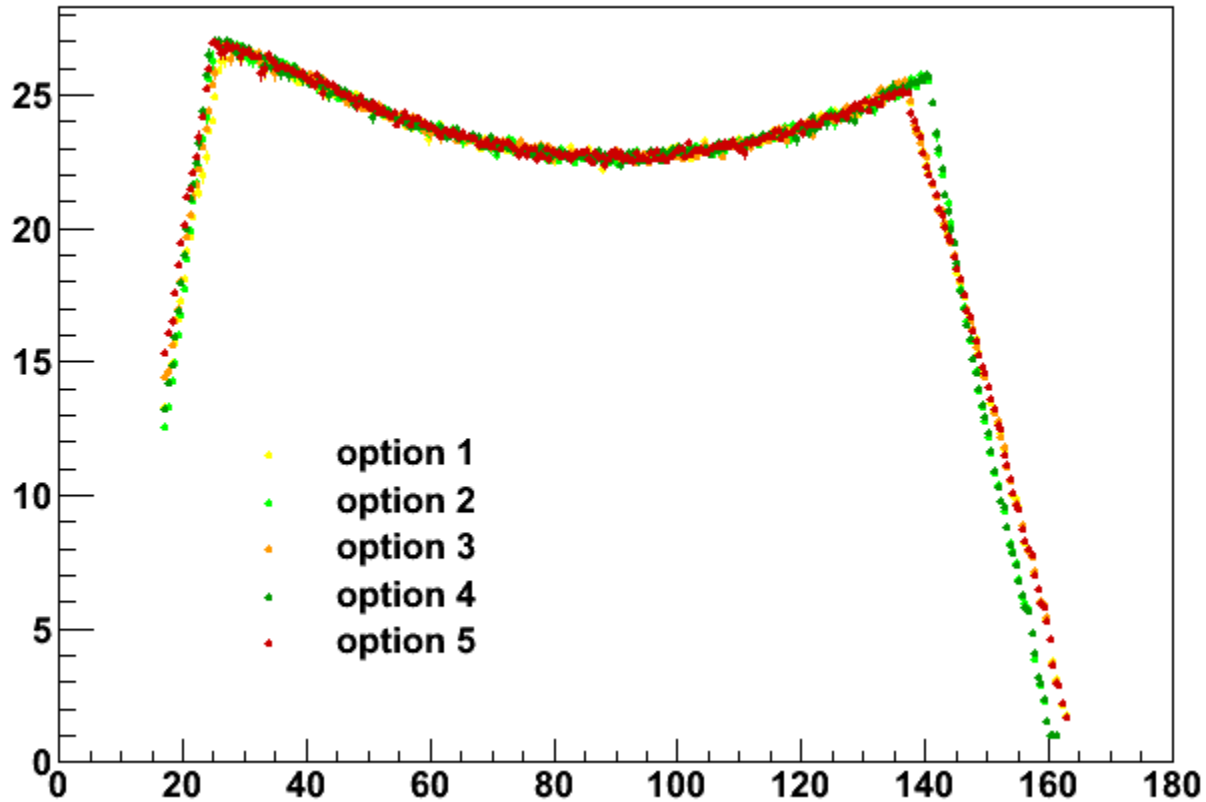
## validation with $p = 4 \text{ GeV}/c$ single particles

single particles generated with:

- $p = 4 \text{ GeV}/c$
- $dP/ d\cos\theta = \text{const}$  [ $\theta = \text{polar angle}$ ]
- $\cos\theta$  in  $[0.3, \pi-0.3]$  rad [SVT angular acceptance]
- 50k events for each configuration

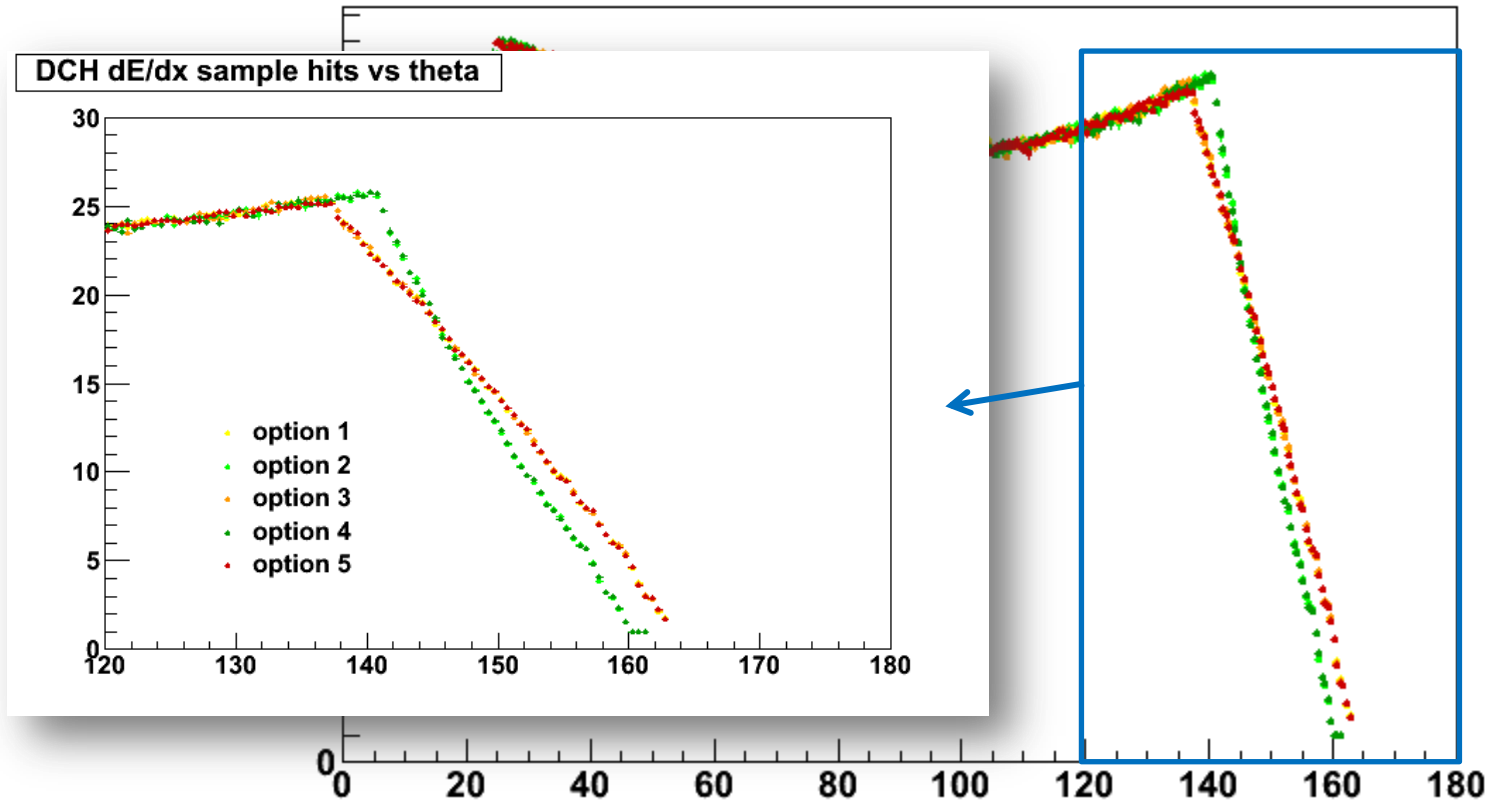
# single $\pi^+$ , $p = 4\text{GeV}/c$ , flat $\cos\theta$

DCH dE/dx sample hits vs theta



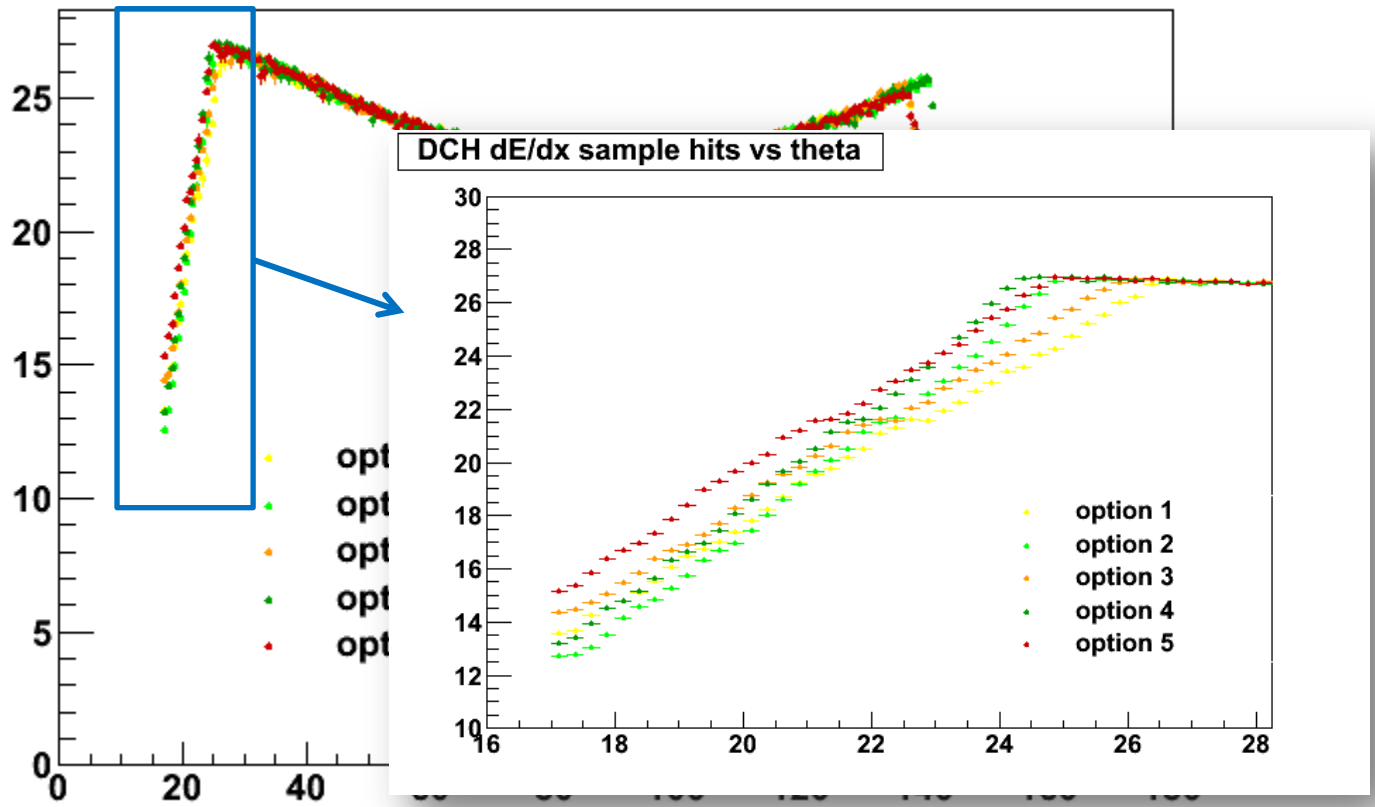
# single $\pi^+$ , $p = 4\text{GeV}/c$ , flat $\cos\theta$

DCH dE/dx sample hits vs theta

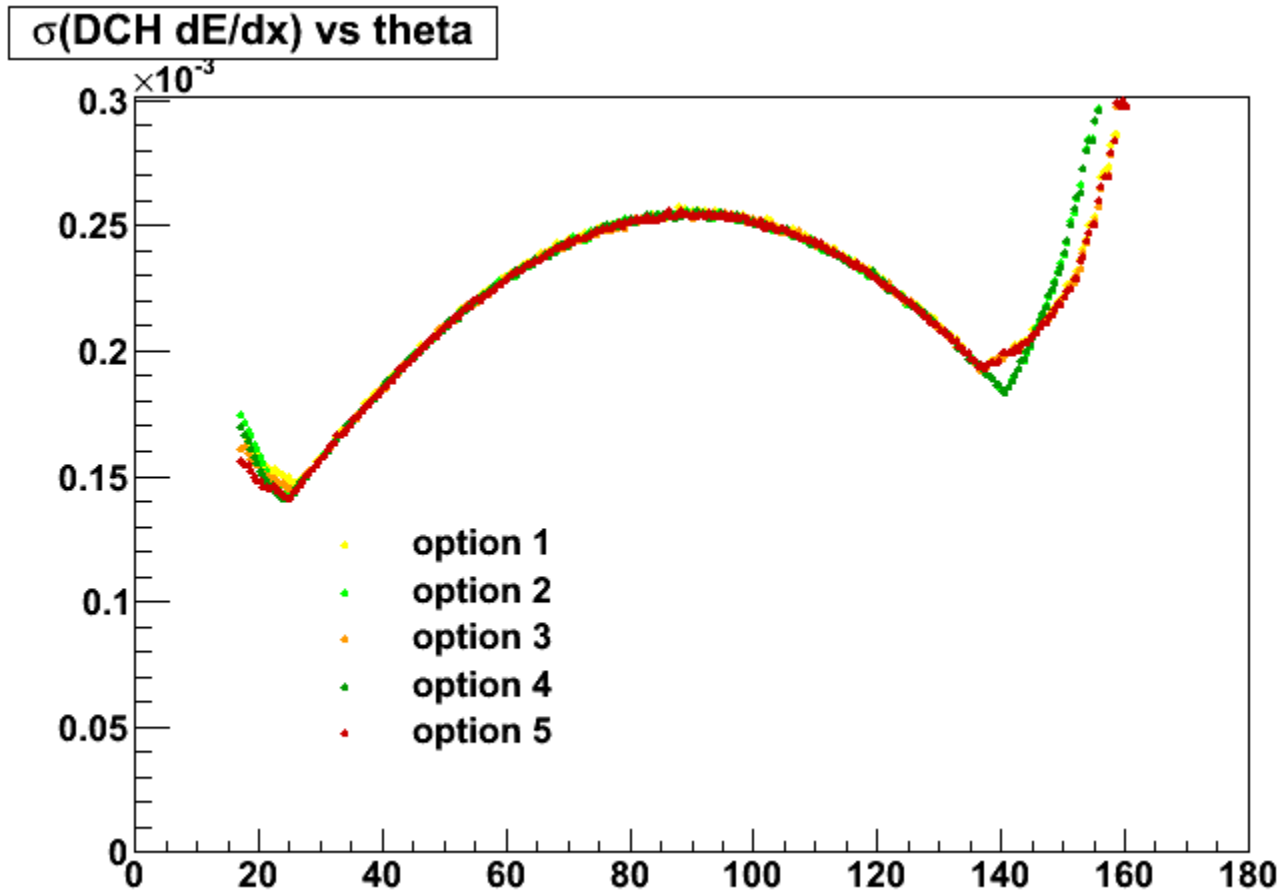


# single $\pi^+$ , $p = 4\text{GeV}/c$ , flat $\cos\theta$

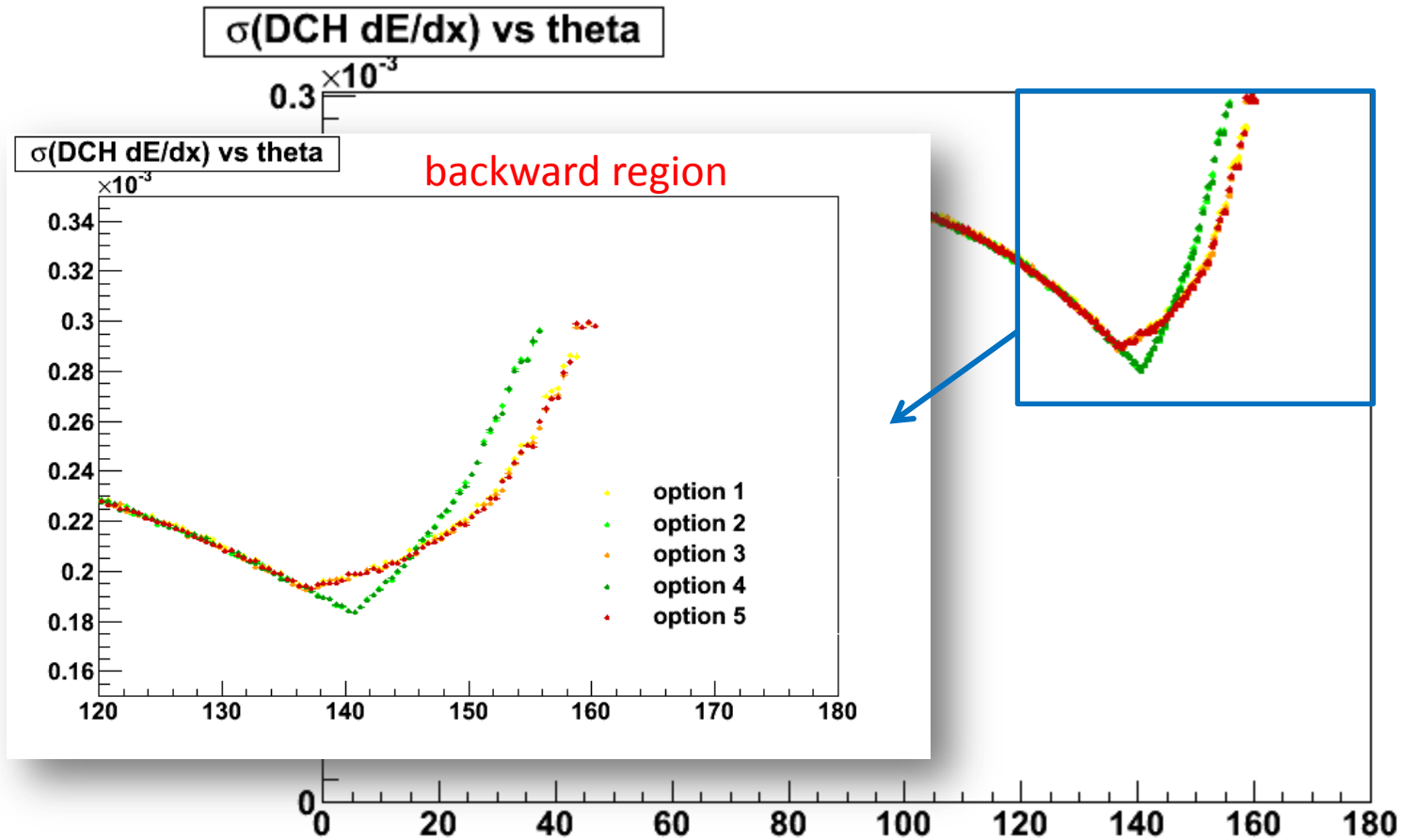
DCH dE/dx sample hits vs theta



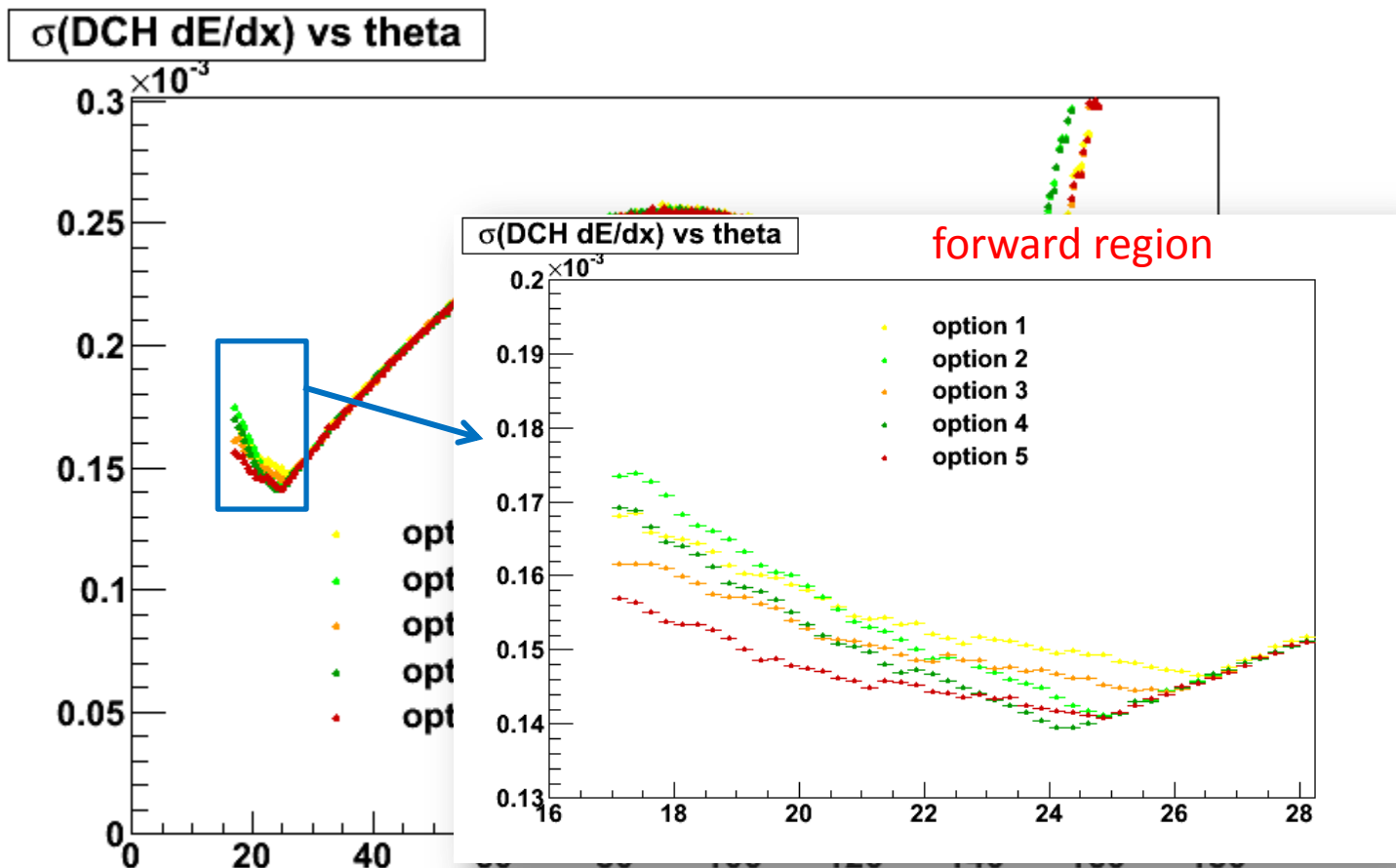
single  $\pi^+$ ,  $p = 4\text{GeV}/c$ , flat  $\cos\theta$



# single $\pi^+$ , $p = 4\text{GeV}/c$ , flat $\cos\theta$

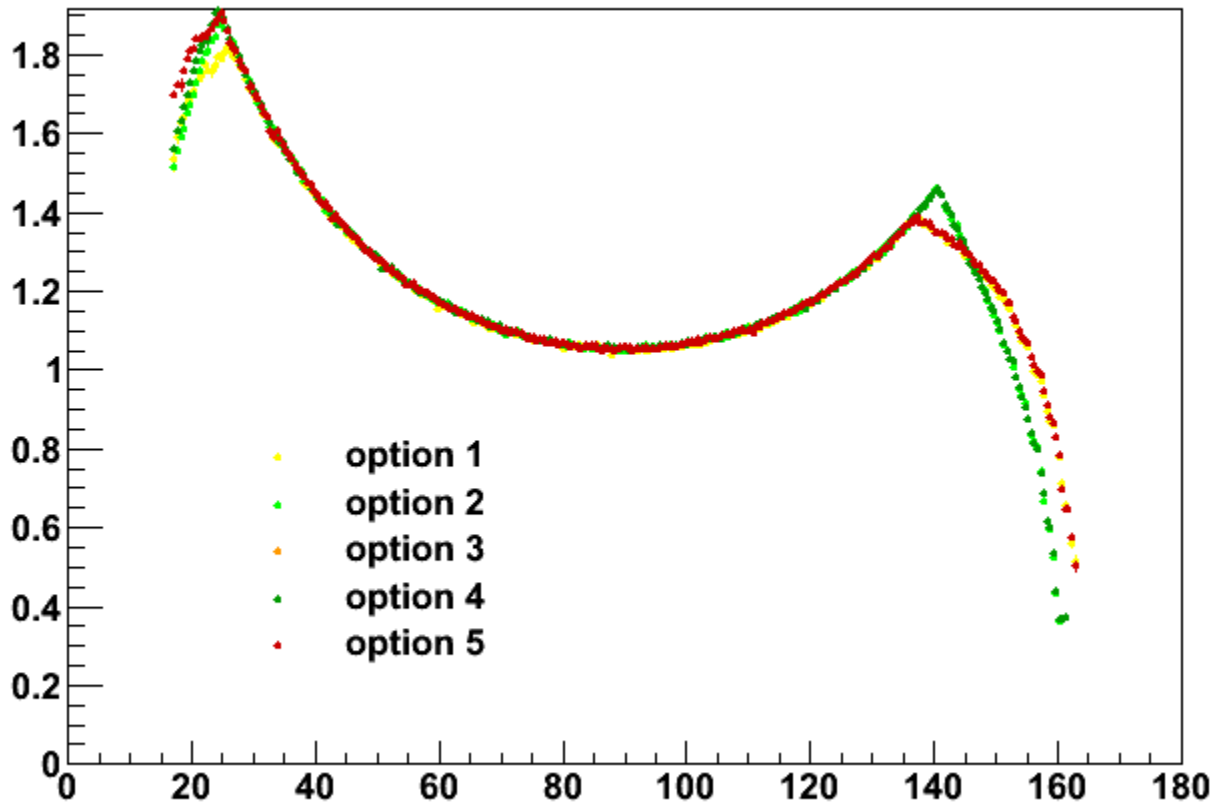


# single $\pi^+$ , $p = 4\text{GeV}/c$ , flat $\cos\theta$



# single $\pi^+$ , $p = 4\text{GeV}/c$ , flat $\cos\theta$

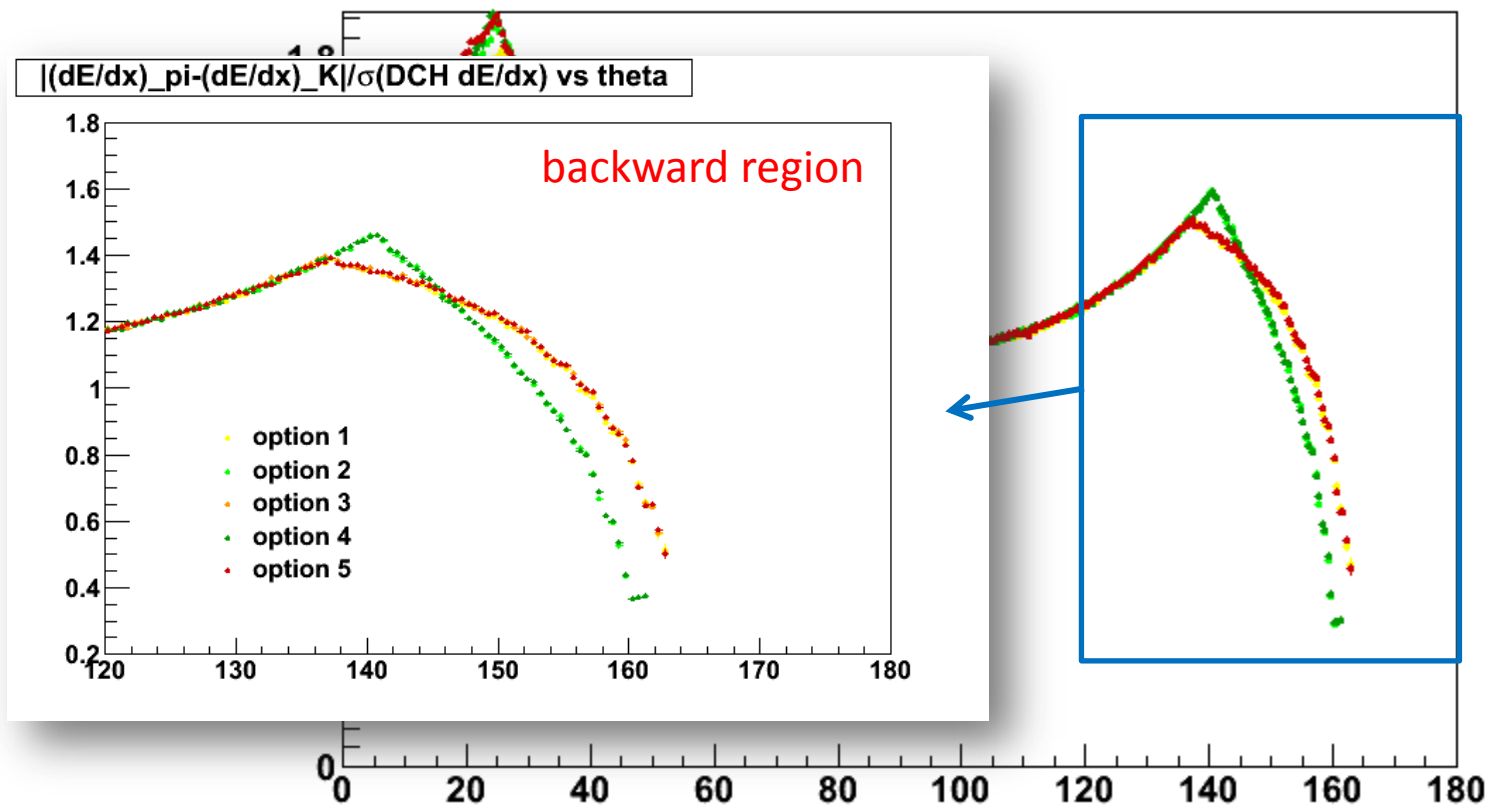
$|(dE/dx)_{\pi} - (dE/dx)_K| / \sigma(\text{DCH } dE/dx)$  vs theta



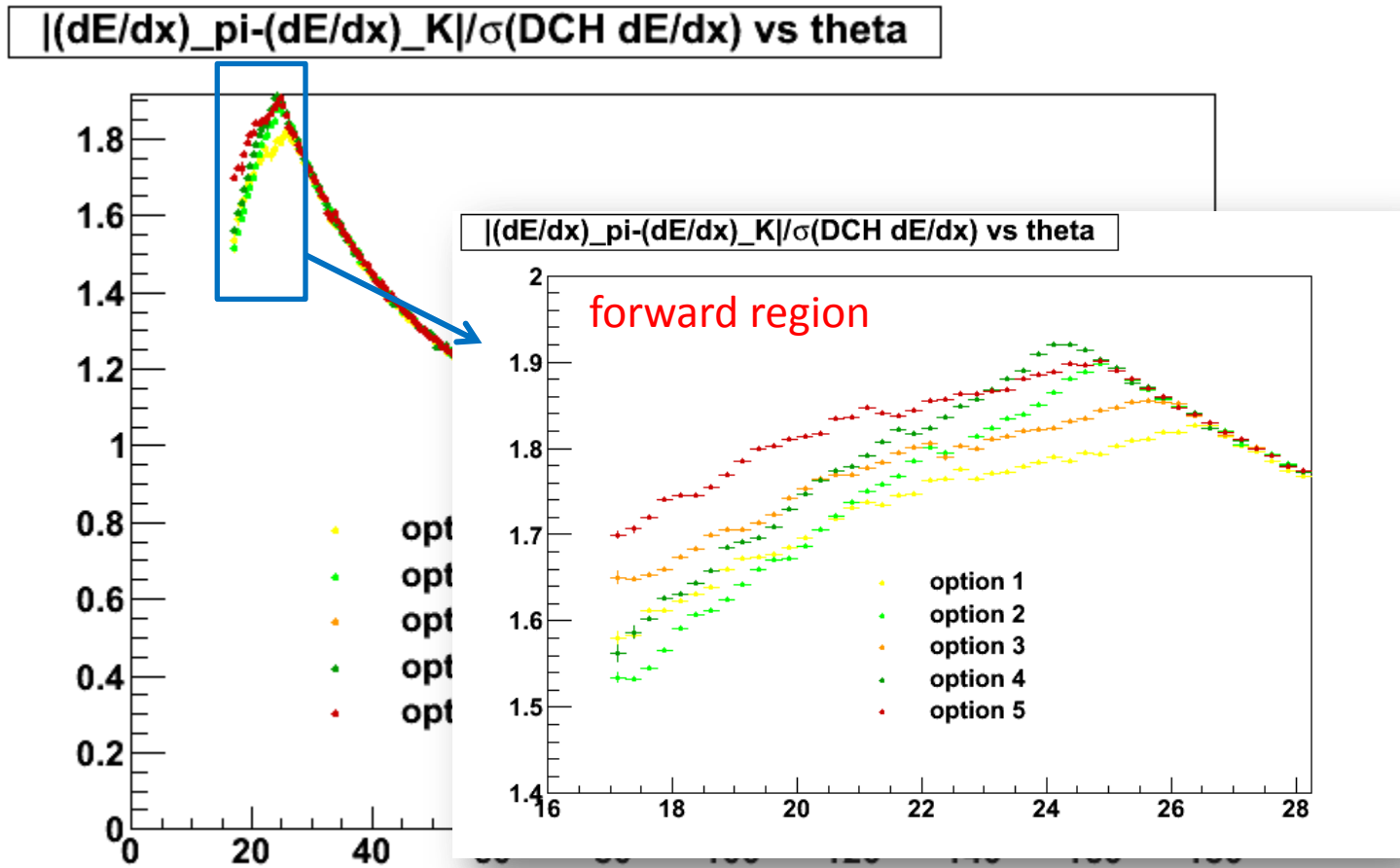


# single $\pi^+$ , $p = 4\text{GeV}/c$ , flat $\cos\theta$

$|(\text{dE/dx})_{\pi} - (\text{dE/dx})_{\text{K}}| / \sigma(\text{DCH dE/dx})$  vs theta



# single $\pi^+$ , $p = 4\text{GeV}/c$ , flat $\cos\theta$



# Part II

## single particles ( $\pi^+$ ) with flat $p$ and $\cos\theta$ distributions

single particles generated with:

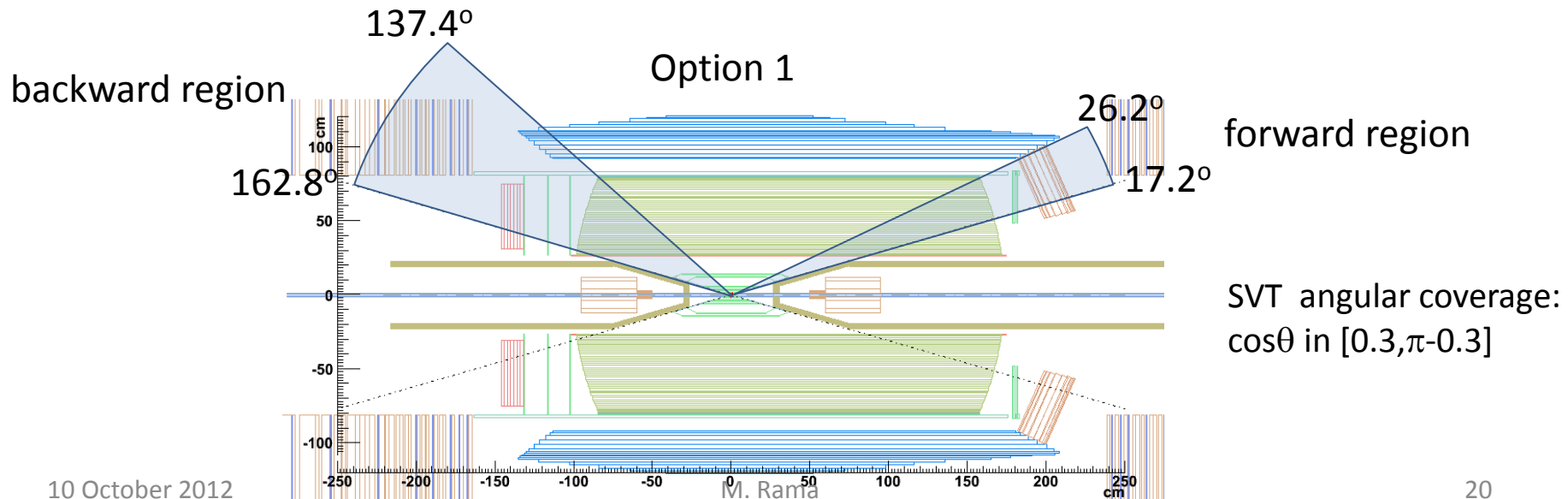
- $p$  in  $[0.1, 4.0]$  GeV/c
- $dP/d\cos\theta = \text{const}$  [ $\theta$  = polar angle]
- $\theta$  in  $[0.30, 0.46]$  rad [DCH forward region] or  
 $\theta$  in  $[2.40, \pi - 0.30]$  rad [DCH backward region]
- 200k events for each configuration

# Part II

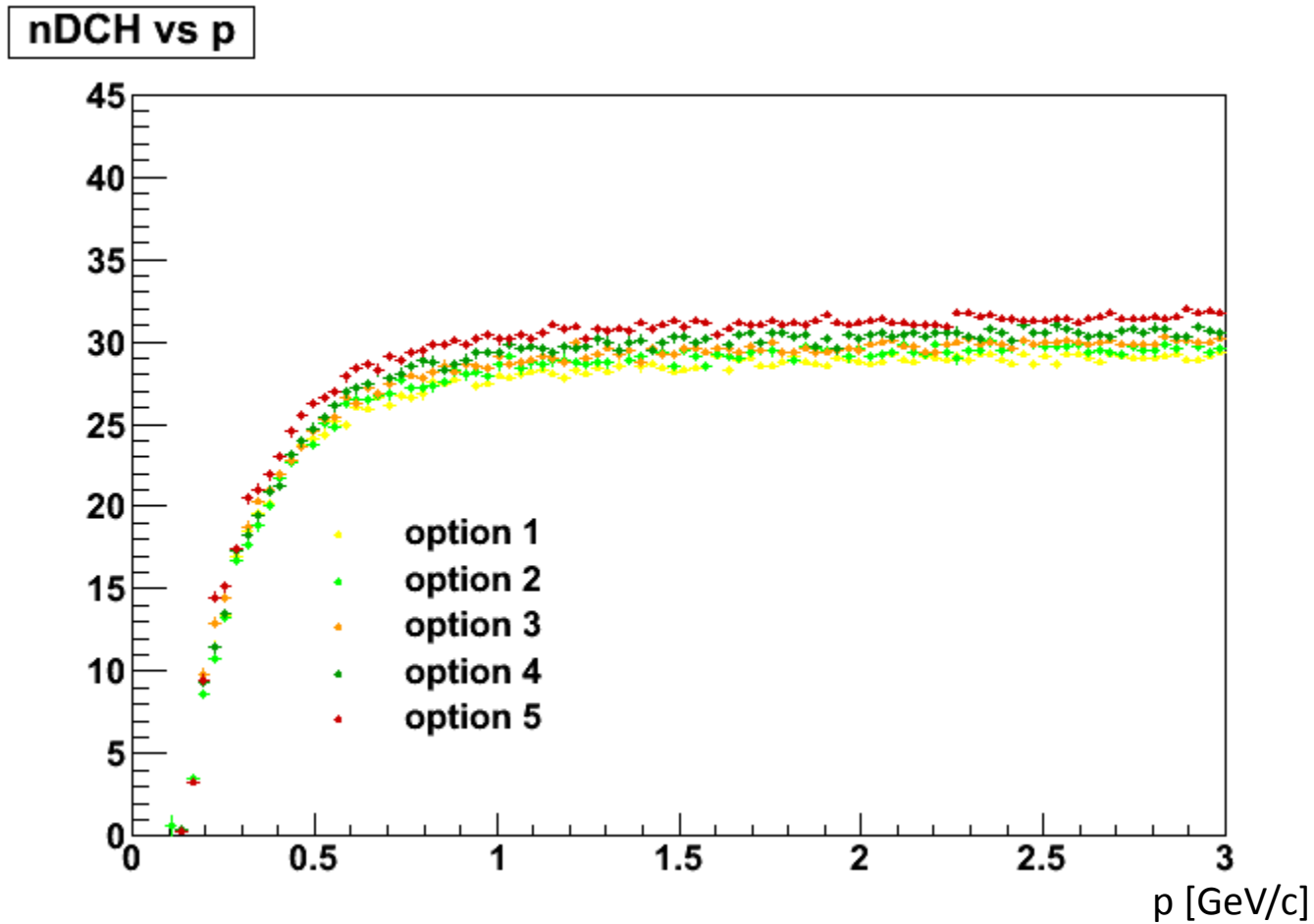
## single particles ( $\pi^+$ ) with flat $p$ and $\cos\theta$ distributions

single particles generated with:

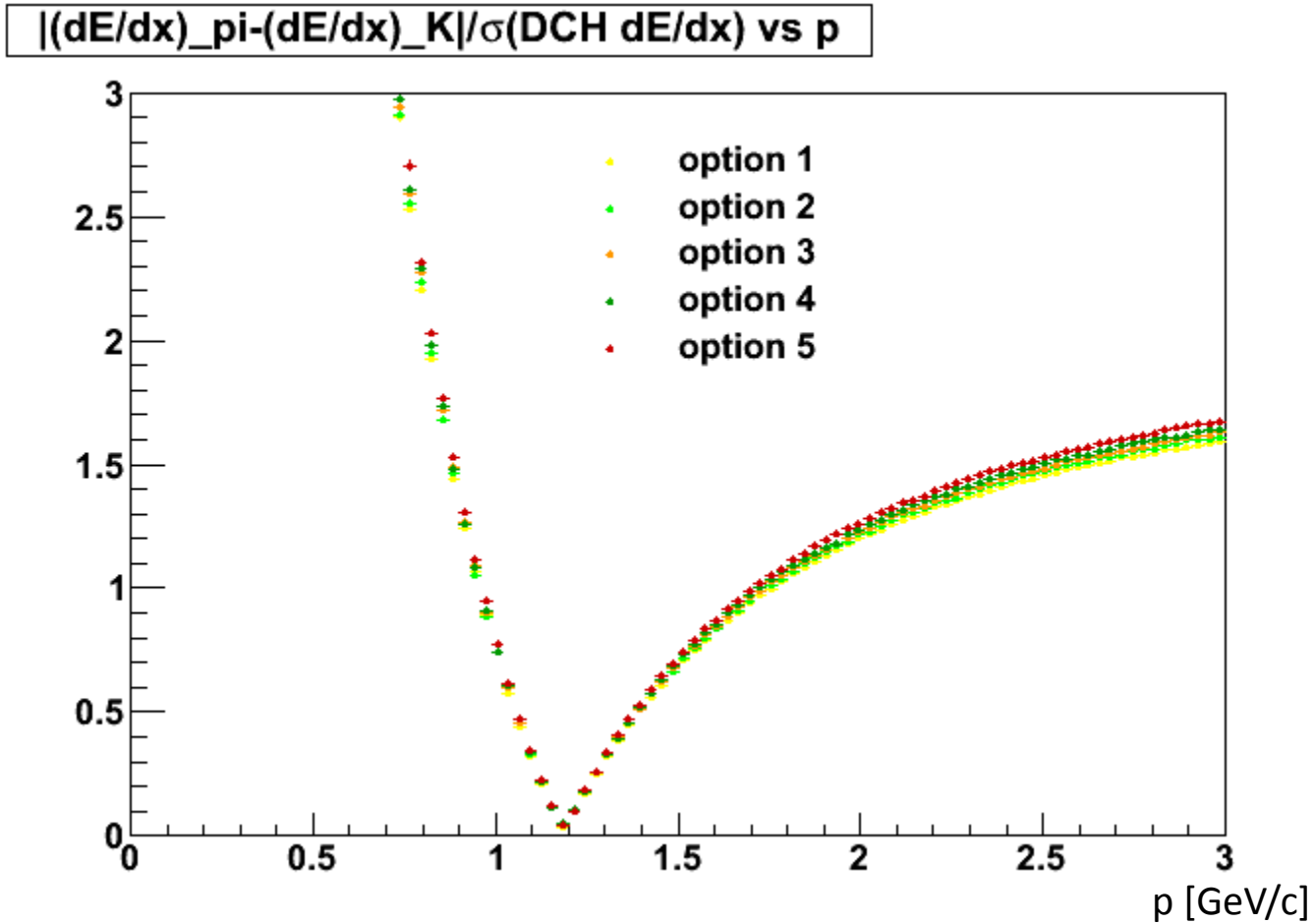
- $p$  in  $[0.1, 4.0]$  GeV/c
- $dP/d\cos\theta = \text{const}$  [ $\theta = \text{polar angle}$ ]
- $\theta$  in  $[0.30, 0.46]$  rad [DCH forward region] or  $\theta$  in  $[2.40, \pi - 0.30]$  rad [DCH backward region]
- 200k events for each configuration



# forward region

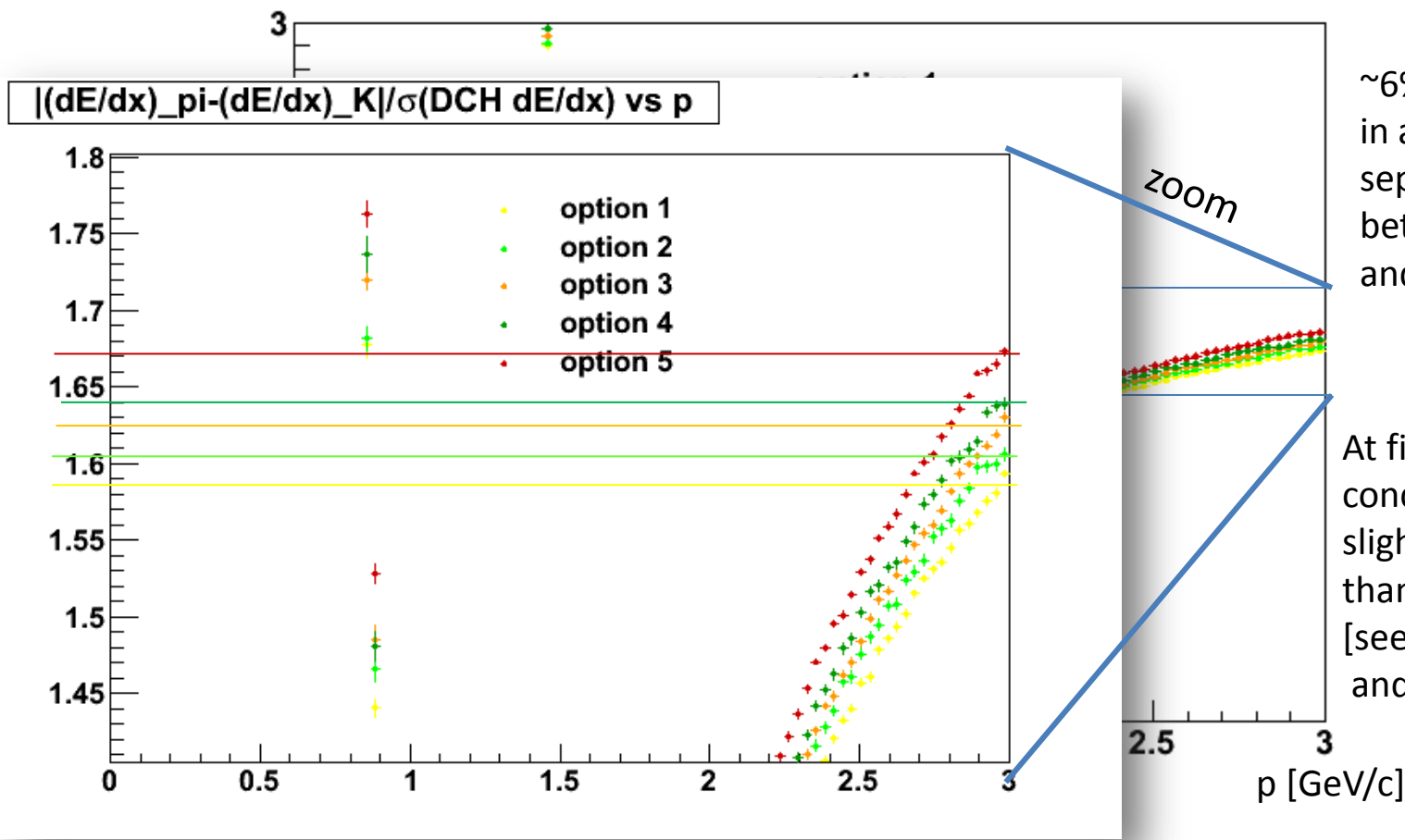


# forward region



# forward region

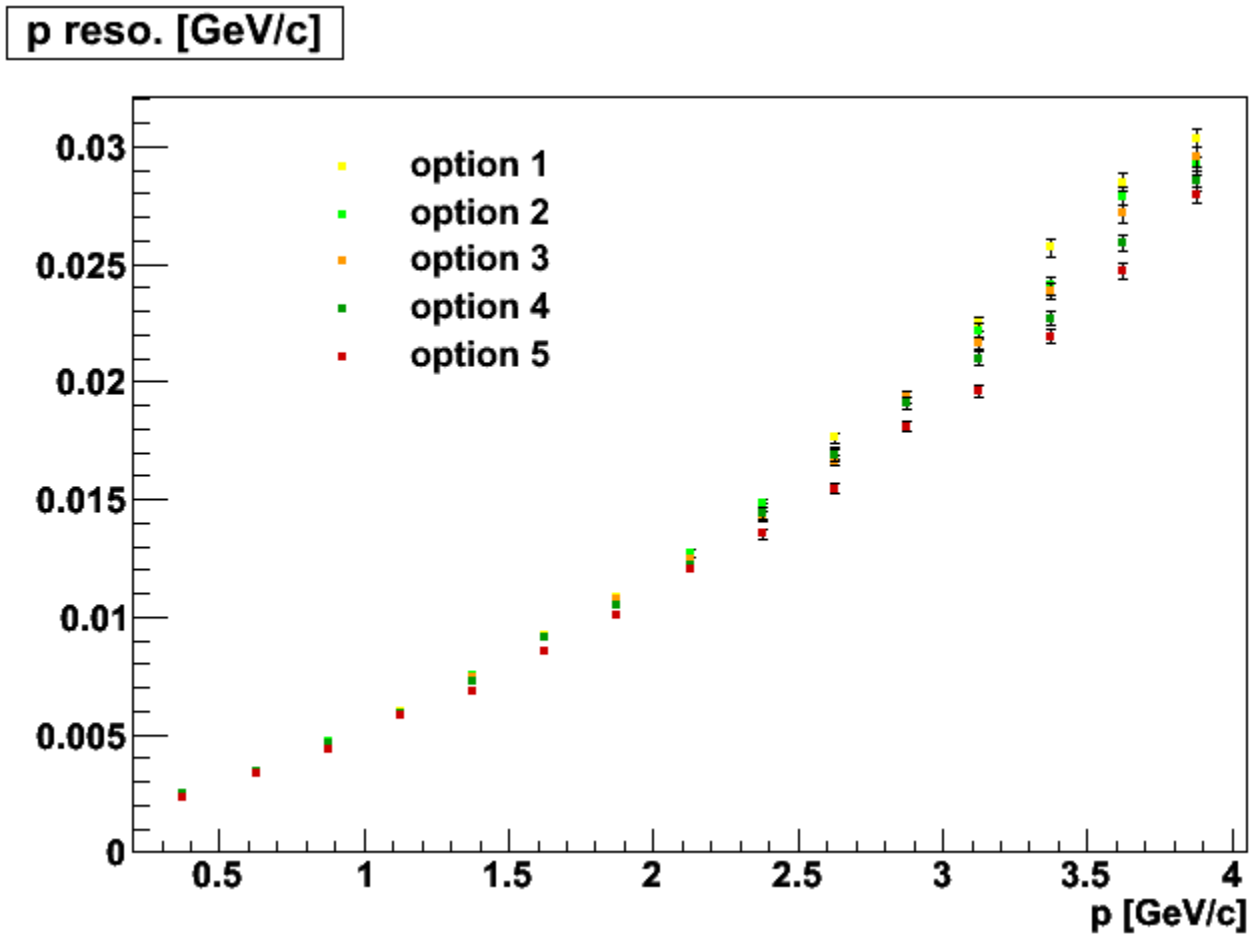
$|(dE/dx)_{\pi} - (dE/dx)_K| / \sigma(\text{DCH } dE/dx) \text{ vs } p$



~6% difference in average  $K/\pi$  separation between opt 1 and opt 5

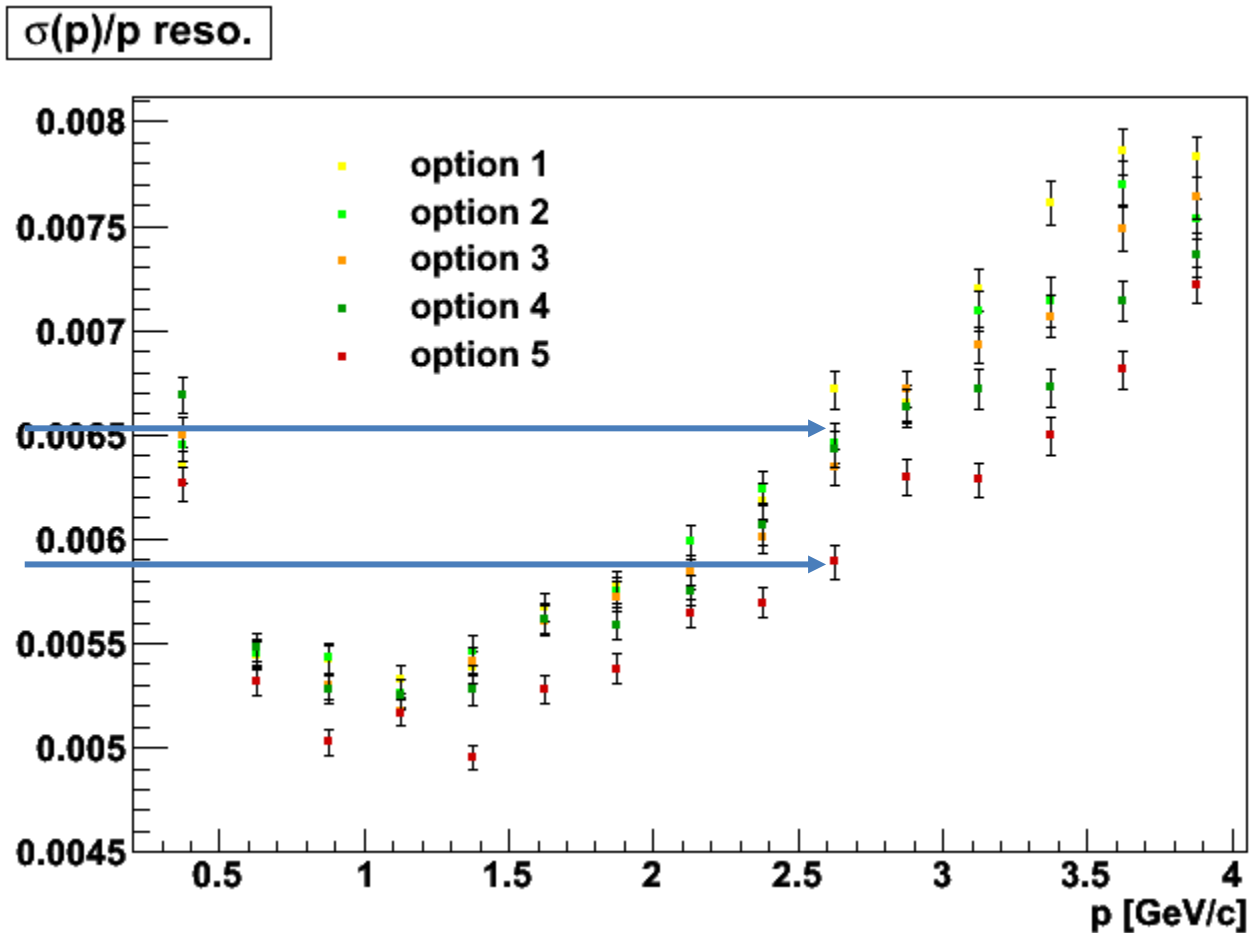
At fixed  $z$  length, concave config slightly better (~1.3%) than convex config. [see opt2 vs opt1 and opt4 vs opt3]

# forward region





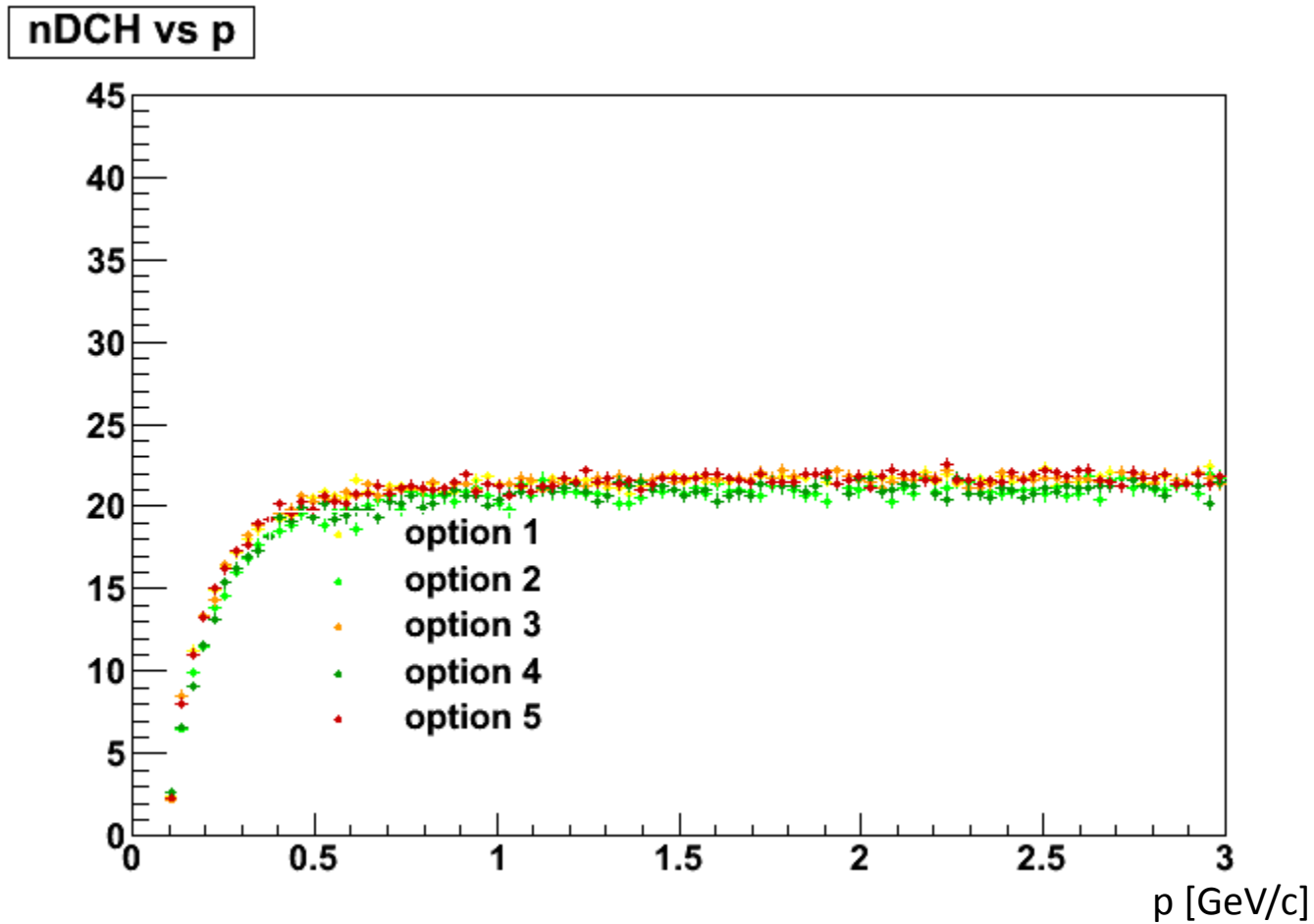
# forward region



$\approx 10\%$   $\sigma(p)/p$   
relative variation  
over different  
configs.

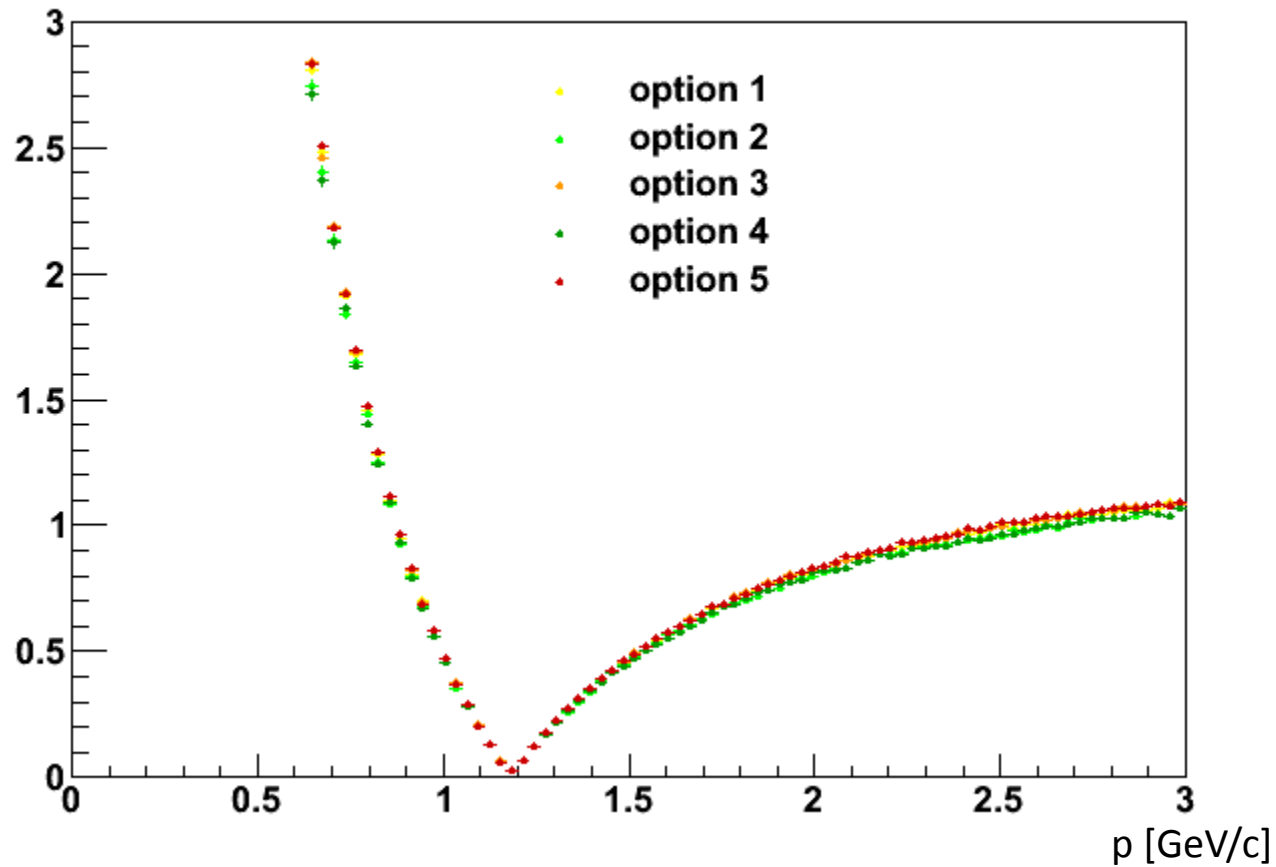
At fixed  $z$  length,  
concave and convex  
configs shows  
similar performance  
within the stat  
uncertainty.

# backward region



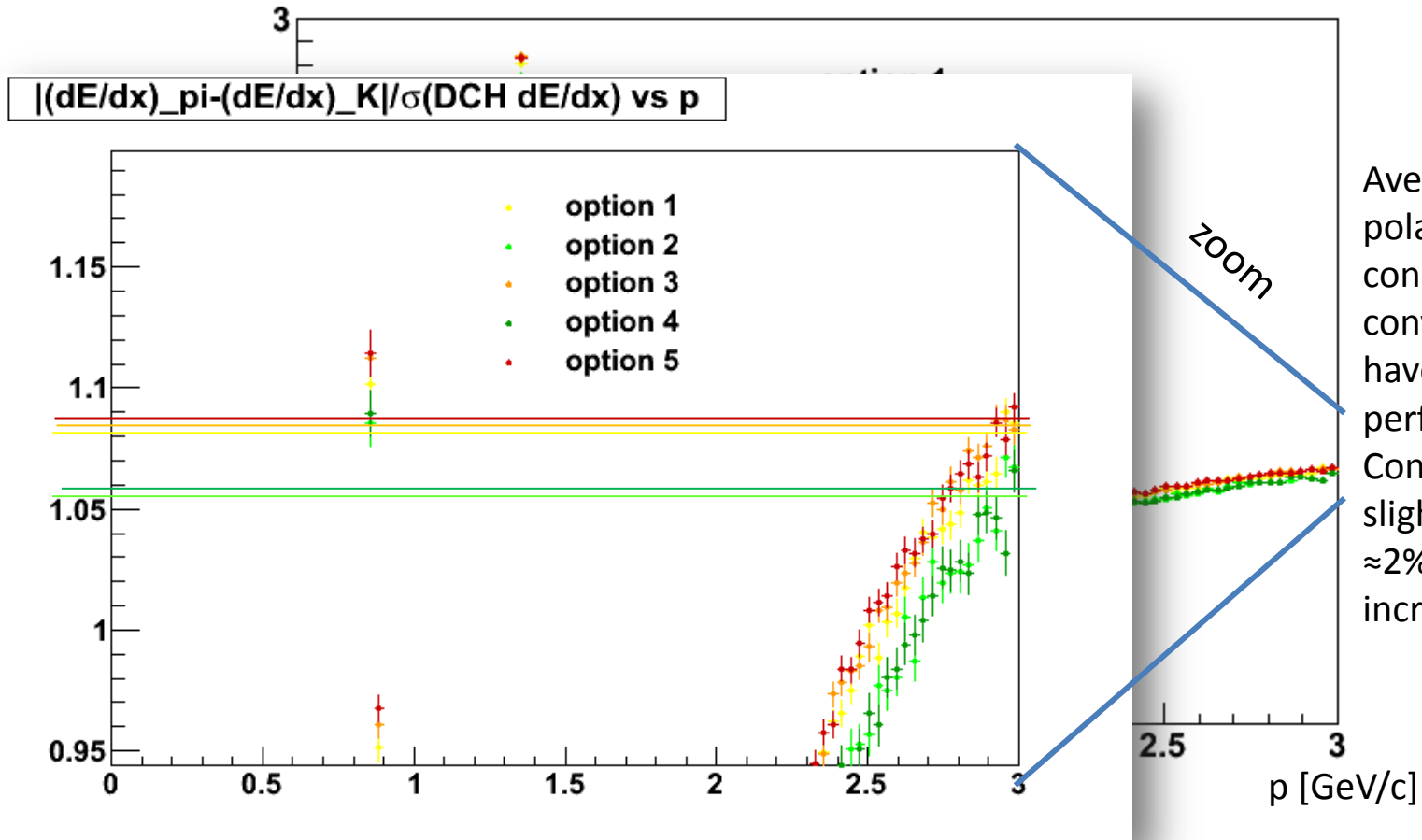
# backward region

$|(dE/dx)_{\pi} - (dE/dx)_K| / \sigma(\text{DCH } dE/dx)$  vs  $p$

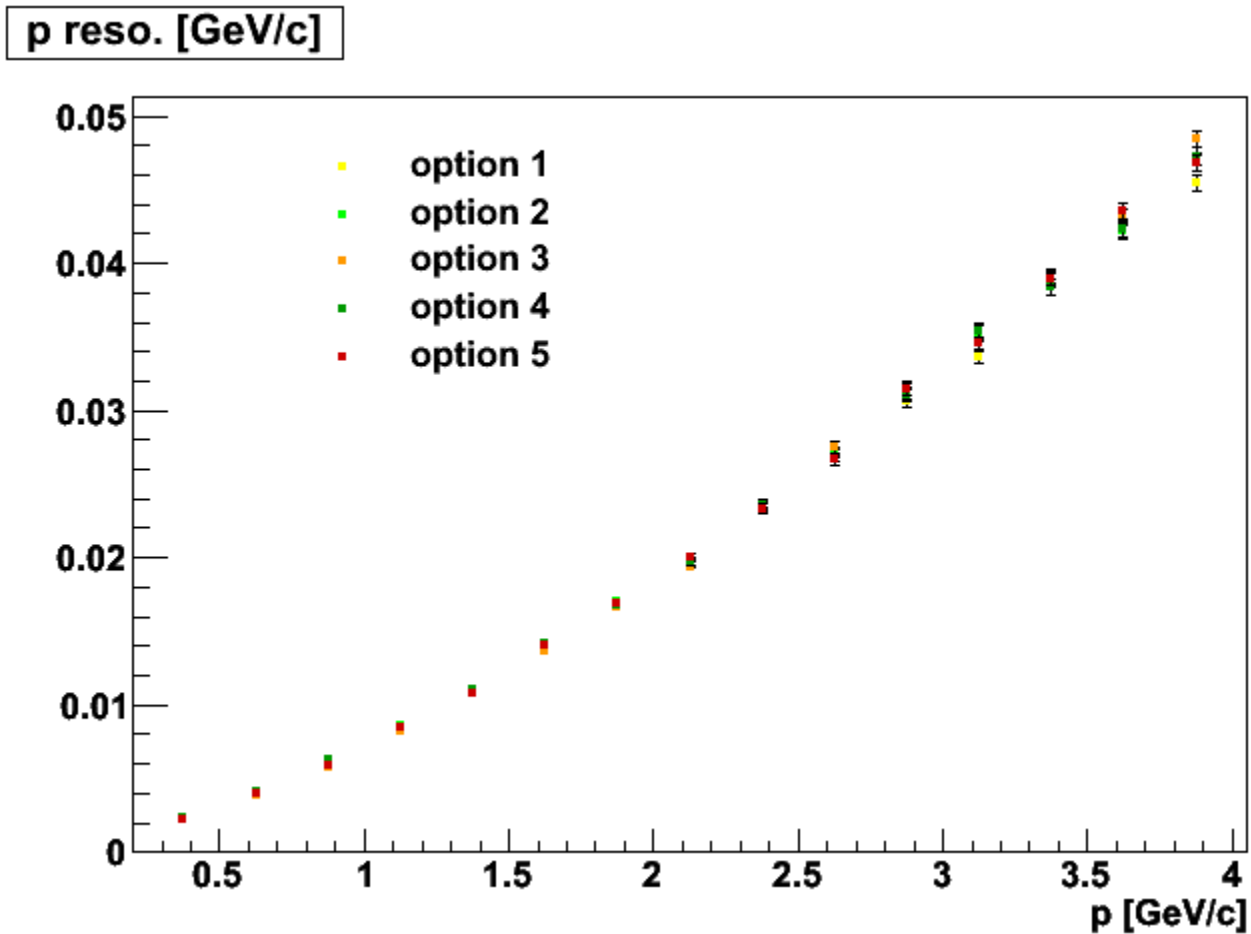


# backward region

$|(dE/dx)_{\pi} - (dE/dx)_K| / \sigma(\text{DCH } dE/dx) \text{ vs } p$

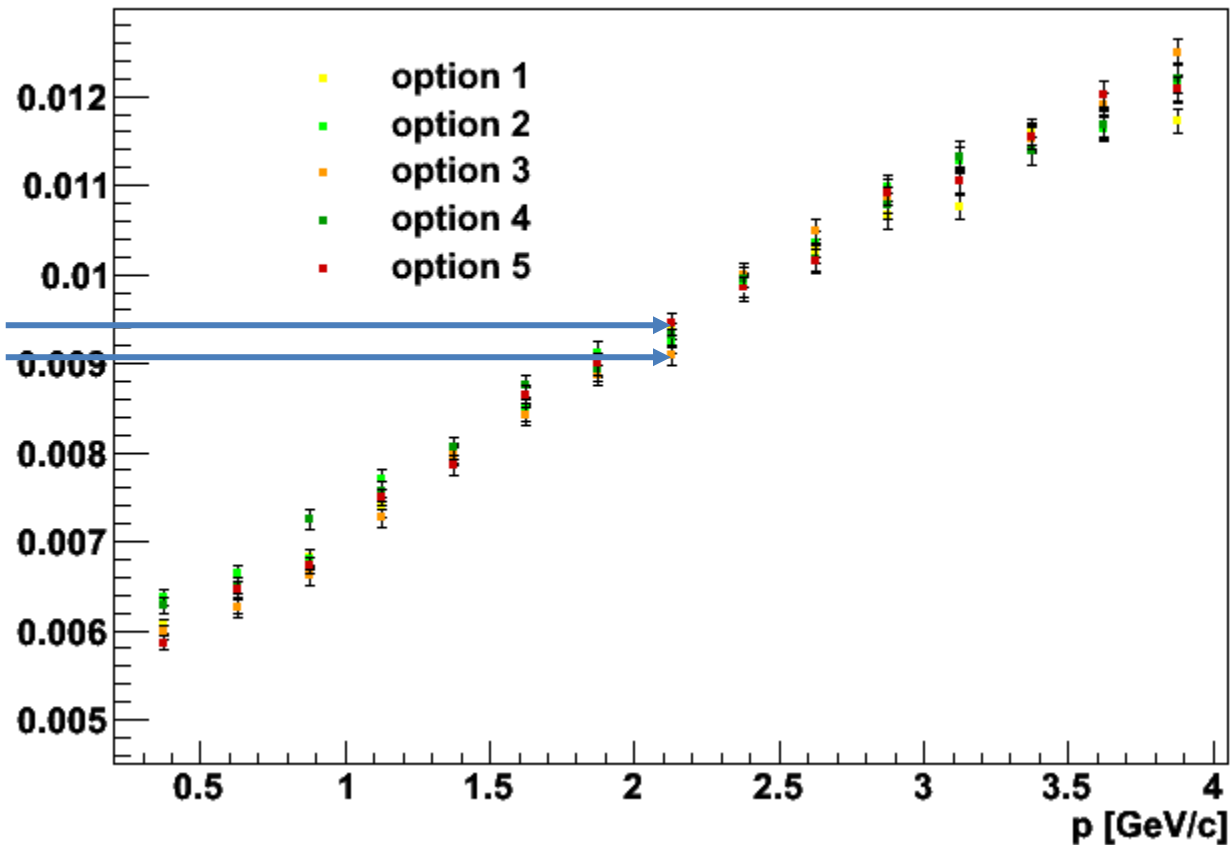


# backward region



# backward region

$\sigma(p)/p$  reso.



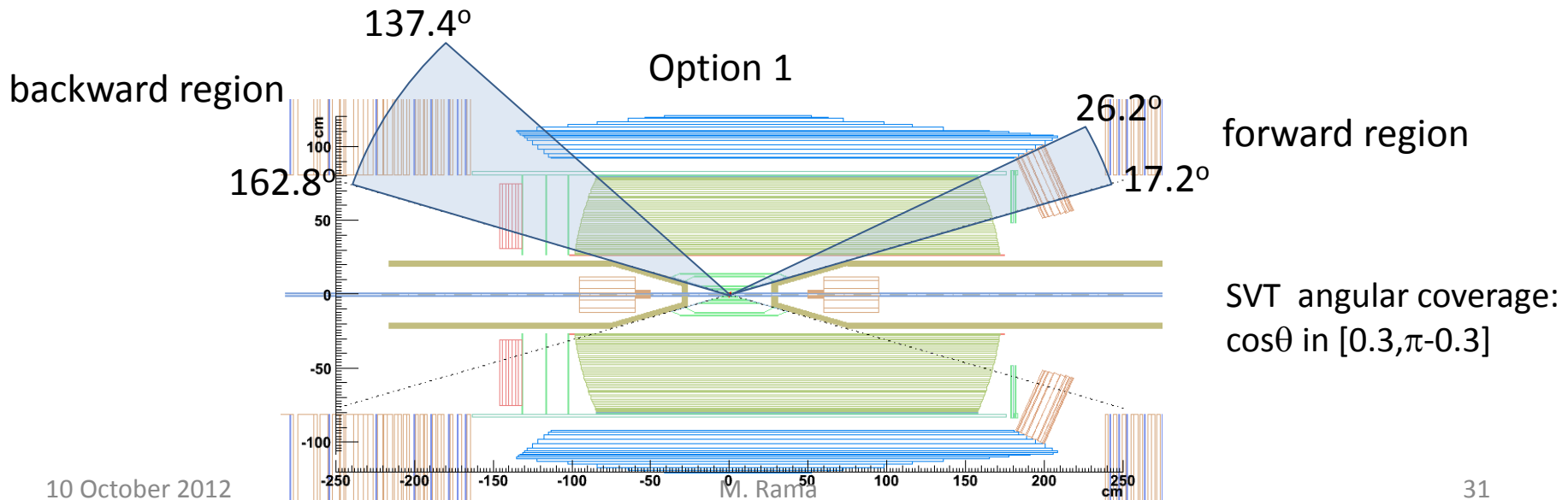
Integrated over the whole bwd region,  $p$  resolutions are similar within a  $\approx 4\%$  relative variation.

# Part III

$$B^0 \rightarrow D^{*-} K^+, D^{*-} \rightarrow \bar{D}^0 K^-, \bar{D}^0 \rightarrow K^+ \pi^-$$

$5 \times 10^4$   $B \rightarrow D^* K$  signal events for each configuration

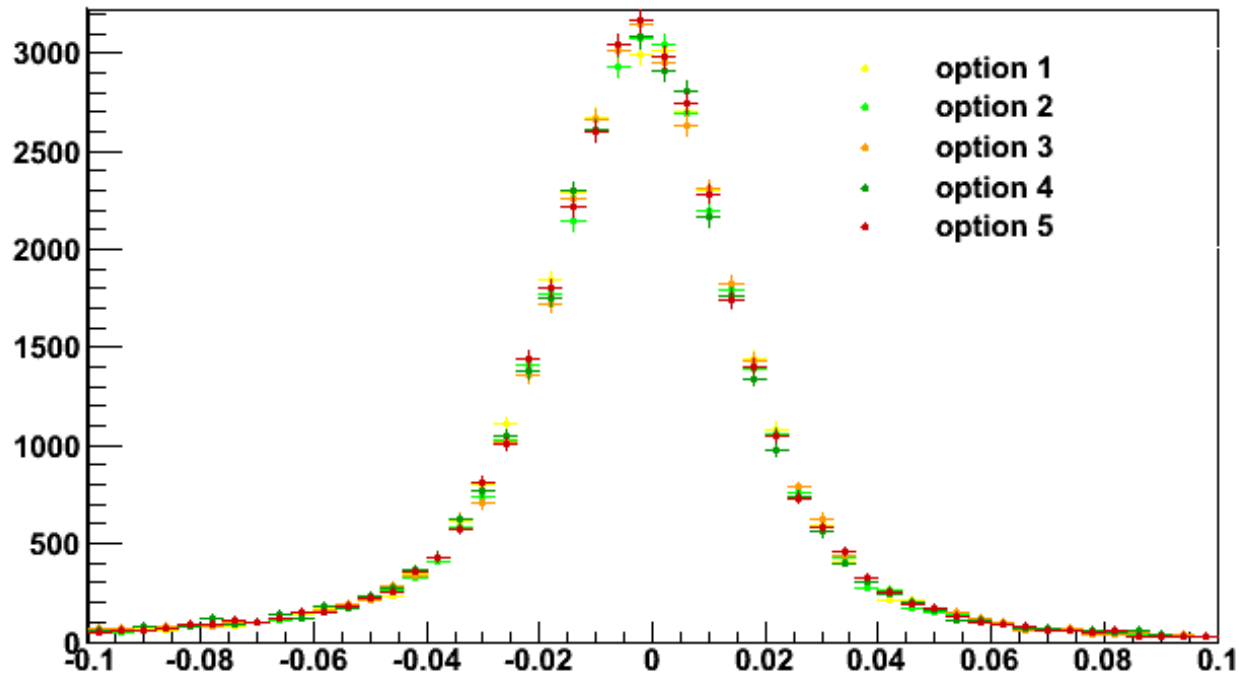
- truth matching required



# $\Delta E$ reconstruction

$$B^0 \rightarrow D^{*-}K^+, D^{*-} \rightarrow \bar{D}^0K^-, \bar{D}^0 \rightarrow K^+\pi^-$$

DeltaE

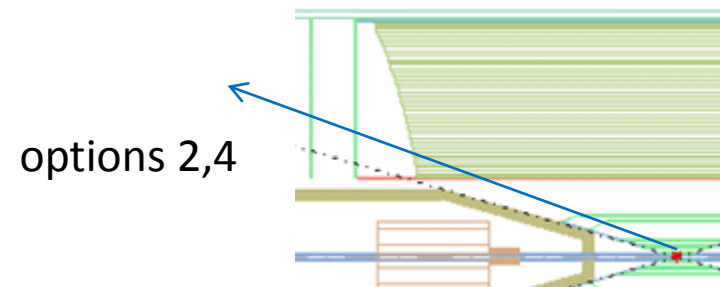
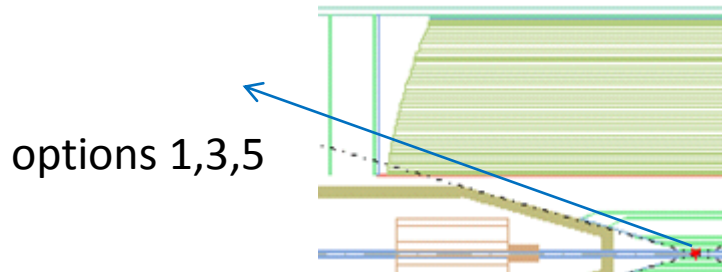




# reconstruction efficiency of $B \rightarrow D^* K$

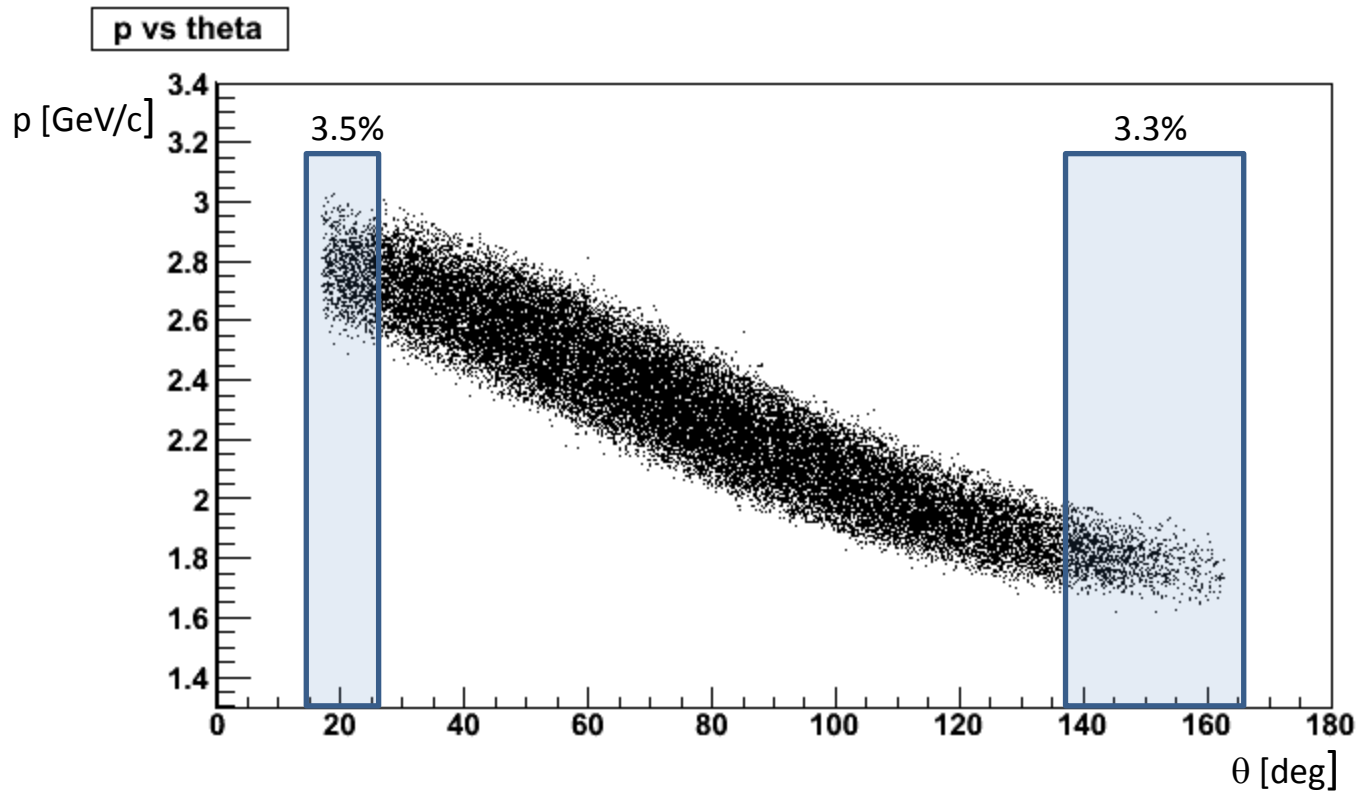
DCH configuration	$B \rightarrow D^* K$ reco efficiency [%] ( $ \Delta E  < 50 \text{ MeV} \sim 2.5\sigma$ )
option 1	$65.4 \pm 0.2$
option 2	$64.4 \pm 0.2$
option 3	$65.1 \pm 0.2$
option 4	$64.6 \pm 0.2$
option 5	$65.3 \pm 0.2$

The (tiny) differences are driven by the backward region:  $\text{eff}[\text{opt}1,3,5] > \text{eff}[\text{opt} 2,4]$



Options 1, 2 and 3 have the same efficiency within  $\approx 0.2\%$

# $p$ vs $\theta$ distribution of prompt kaons ( $B \rightarrow D^* K$ )



## selected samples

forward region: 1213 (3.5%)

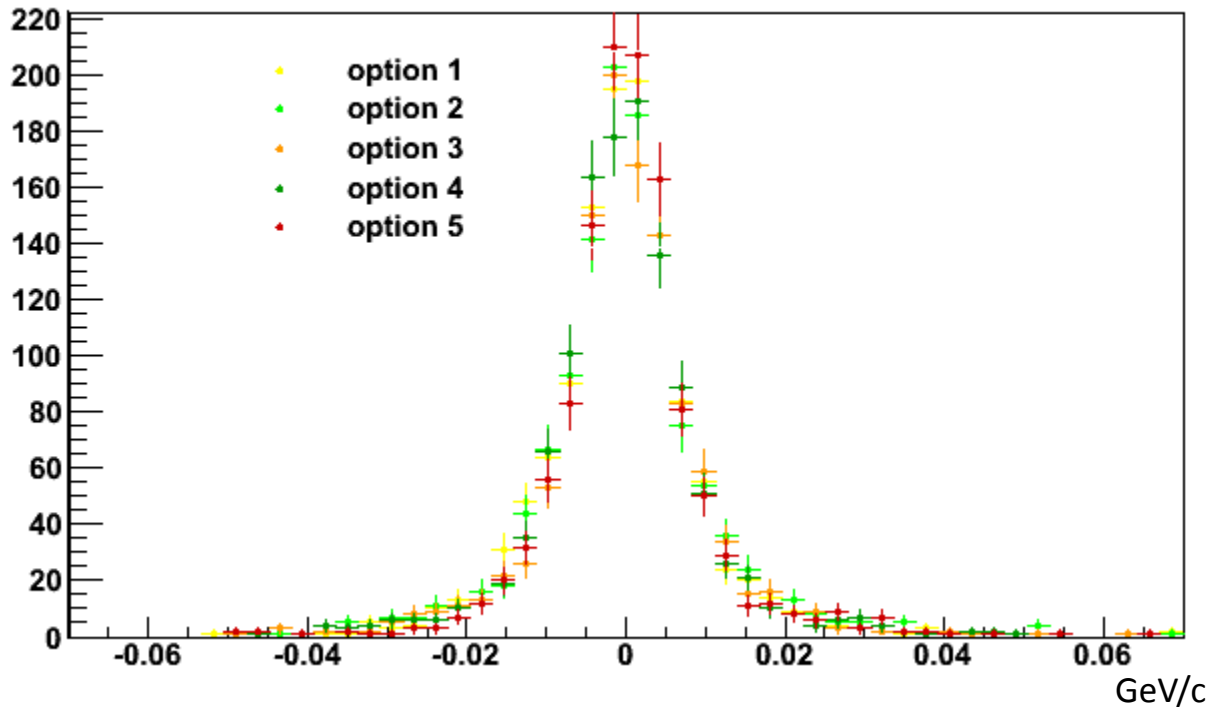
barrel region: 32242 (93.2%)

backward region: 1157 (3.3%)

# forward region

pt resolution for prompt kaons in forward region

pt reso



Option 5 is visibly better.  
Differences in opt1-4 are not evident.

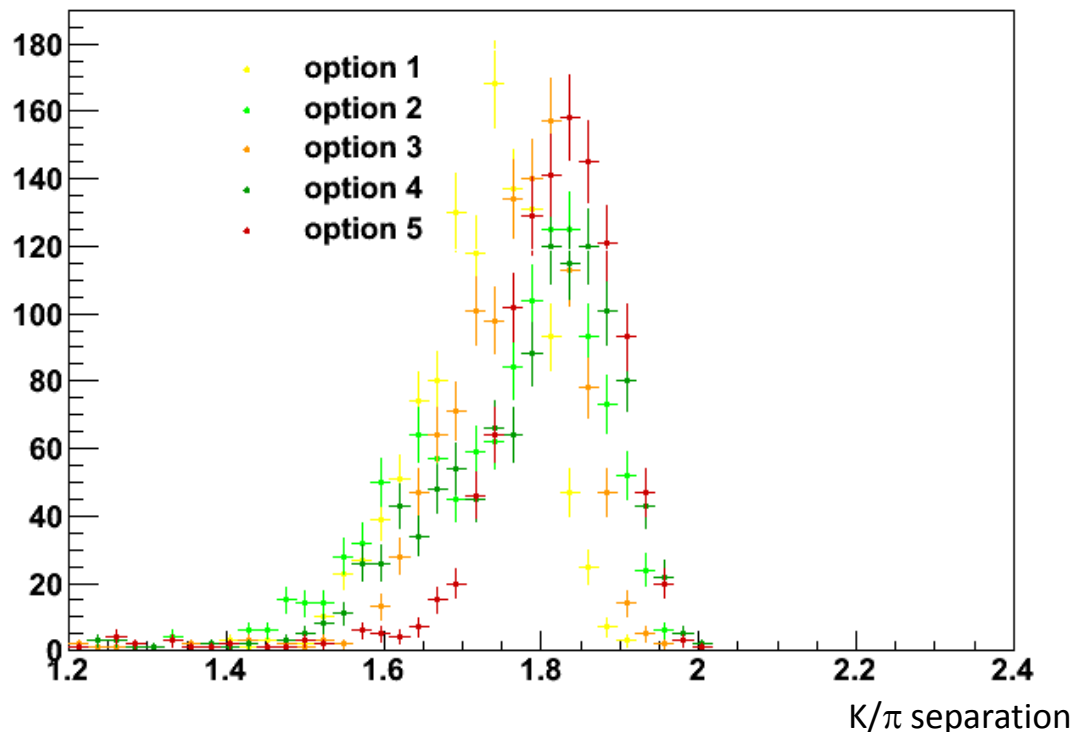
# forward region

$$K/\pi \text{ separation} \equiv \frac{|(dE/dx)_\pi - (dE/dx)_K|}{\sigma(dE/dx)}$$

$(dE/dx)_h =$  expected  $dE/dx$  in the  $h$  hypothesis

$\sigma(dE/dx) =$   $dE/dx$  measurement error

$|(\text{dE/dx})_{\text{pi}} - (\text{dE/dx})_{\text{K}}| / \sigma(\text{DCH dE/dx})$  forward



config	$\mu \pm \text{RMS}/\sqrt{N}$
1	$1.723 \pm 0.002$
2	$1.751 \pm 0.003$
3	$1.767 \pm 0.003$
4	$1.787 \pm 0.003$
5	$1.822 \pm 0.003$

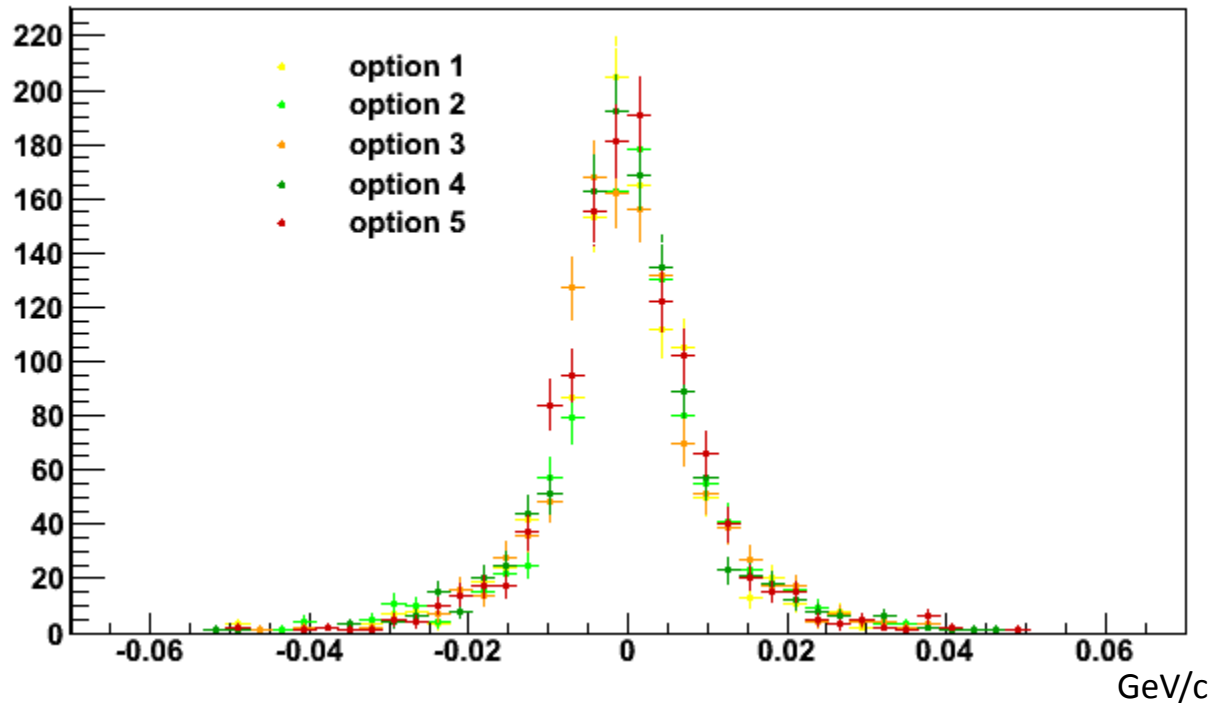
The pattern  $sep1 < sep2 < sep3 < sep4 < sep5$  is visible. Differences are tiny.

At fixed  $z$  length, concave config slightly better ( $\approx 1\%$ ) than convex config.  
[see opt2 vs opt1 and opt4 vs opt3]

# backward region

pt resolution for prompt kaons in backward region

pt reso



# backward region

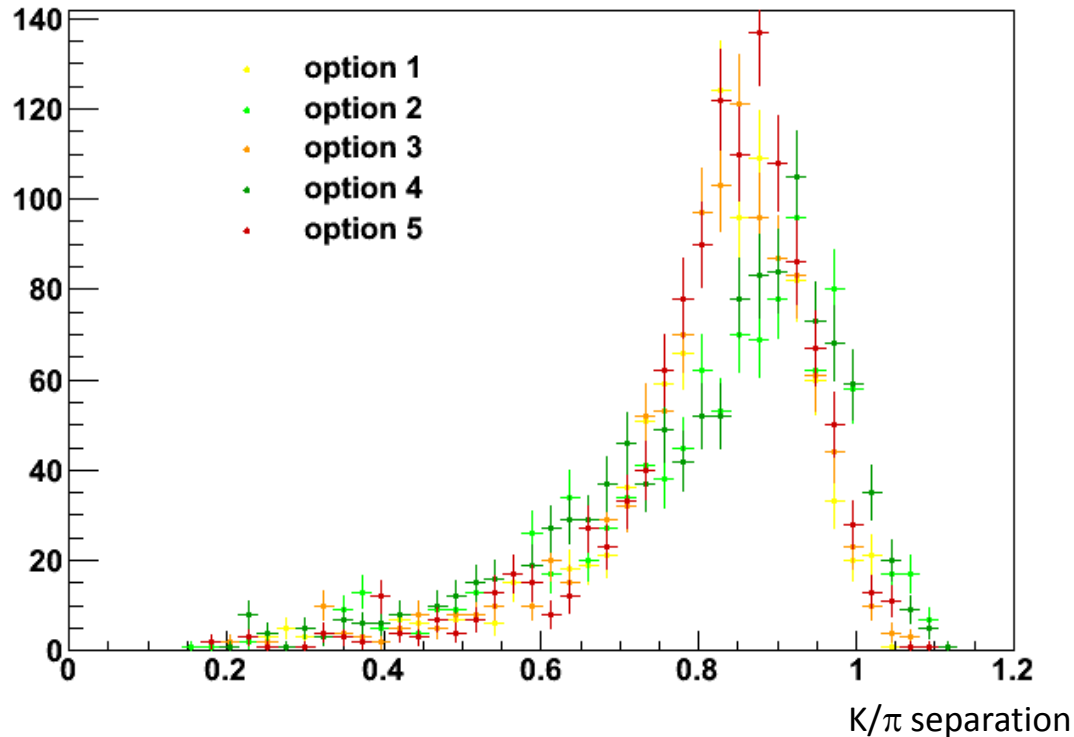
$$K/\pi \text{ separation} \equiv \frac{|(dE/dx)_\pi - (dE/dx)_K|}{\sigma(dE/dx)}$$

$(dE/dx)_h =$  expected  $dE/dx$  in the  $h$  hypothesis

$\sigma(dE/dx) =$   $dE/dx$  measurement error

config	$\mu \pm RMS/\sqrt{N}$
1	$0.801 \pm 0.004$
2	$0.812 \pm 0.005$
3	$0.802 \pm 0.004$
4	$0.808 \pm 0.005$
5	$0.816 \pm 0.004$

**| $(dE/dx)_\pi - (dE/dx)_K|/\sigma(DCH \text{ } dE/dx)$  backward**



Average  $K/\pi$  separations consistent within  $\approx 0.5\%$

# Conclusions

- 5 options for the DCH endcaps have been compared. They differ in shape and z position.
- Differences in performance are generally small, as expected.
- Forward region
  - K/ $\pi$  separation: At fixed z position, the concave shape shows slightly better performance ( $\approx 1\%$  relative gain).
  - p resolution:  $\approx 10\%$   $\sigma(p)/p$  variation over different configs. Consistent with previous estimates of  $\sim 1\%$  per cm of DCH length[1]. At fixed z length, concave and convex configs shows similar performance within the stat uncertainty (2-3%).
  - B $\rightarrow$ D\*K: Possible differences in absolute (relative) reco efficiency due to track reconstruction and  $\Delta E$  resolution are below 0.2% (0.3%) among different configs.
- Backward region
  - K/ $\pi$  separation: Using single particles generated with flat  $\cos\theta$  and p distributions, and averaging over the bwd region, the convex configuration shows slightly better performance ( $\approx 2\%$ ). Using prompt kaons from B $\rightarrow$ D\*K, concave and convex configurations are consistent within 0.5%.
  - p resolution: Integrated over the whole bwd region, p resolutions are equal within a  $\approx 4\%$  relative uncertainty.
  - B $\rightarrow$ D\*K: convex configuration shows slightly larger B $\rightarrow$ D\*K reco efficiency: 0.8% (1.2%) absolute (relative) efficiency gain.

[1] <http://agenda.infn.it/getFile.py/access?contribId=74&sessionId=11&resId=0&materialId=slides&confId=2902>

[2] <http://agenda.infn.it/getFile.py/access?contribId=133&sessionId=19&resId=0&materialId=slides&confId=1165>

# convex vs concave shape summary

Summary of results concerning the comparison between the concave and convex shapes with a given length (i.e., option1 vs option2 or option3 vs option4)

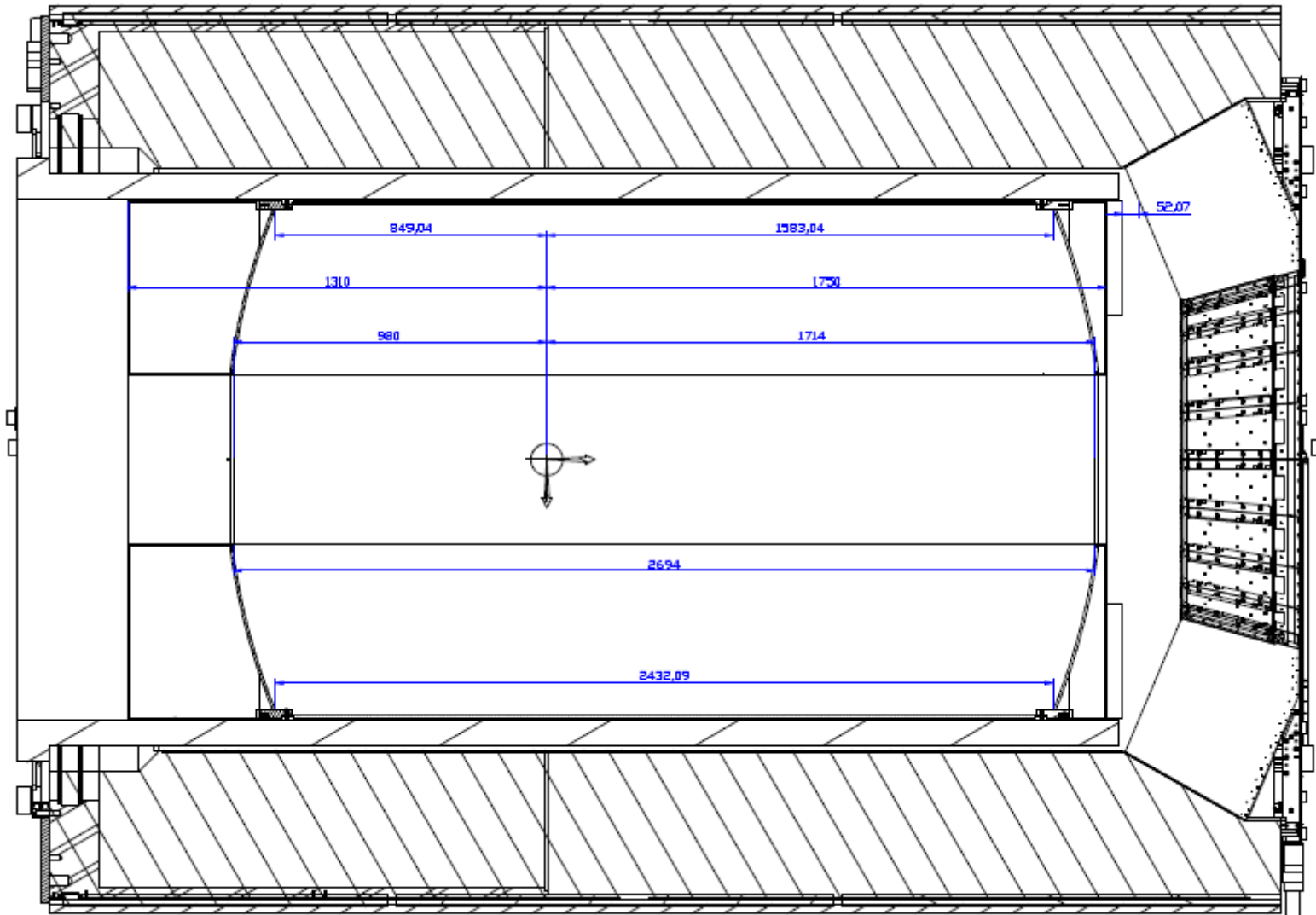
	forward region	backward region
$K/\pi$ separation	concave +1% w.r.t. convex	With single particles (flat $\cos\theta$ ): convex +2% w.r.t. concave With prompt K from $B \rightarrow D^*K$ : same separation within 0.5%. (*)
$\sigma(p)/p$	same resolution within 2-3% relative uncertainty (stat limited)	same resolution within $\approx 4\%$ relative uncertainty (stat limited)
$B \rightarrow D^*K$ reco. eff.	same reco. eff. within 0.3% relative uncertainty (stat limited)	convex +1.2% relative increase w.r.t. concave

(\*) The  $K/\pi$  separation depends on both the polar angle (see for example slide 17) and  $p$ . Therefore, results for particle samples with different polar angle and  $p$  distributions can vary.



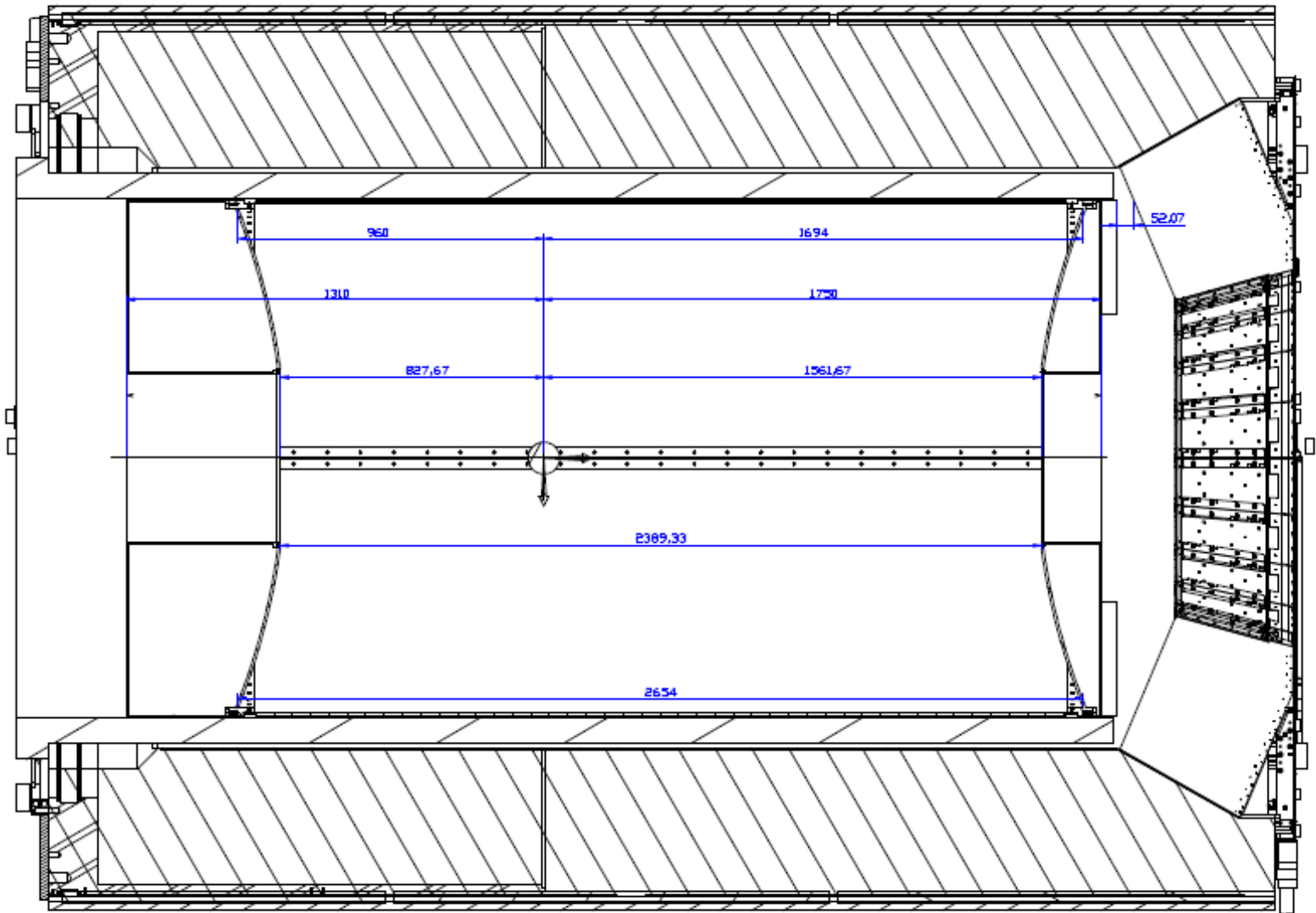
backup

1) CONVEX dimensions -1310 +1750



Drawing from Stefano Lauciani, LNF

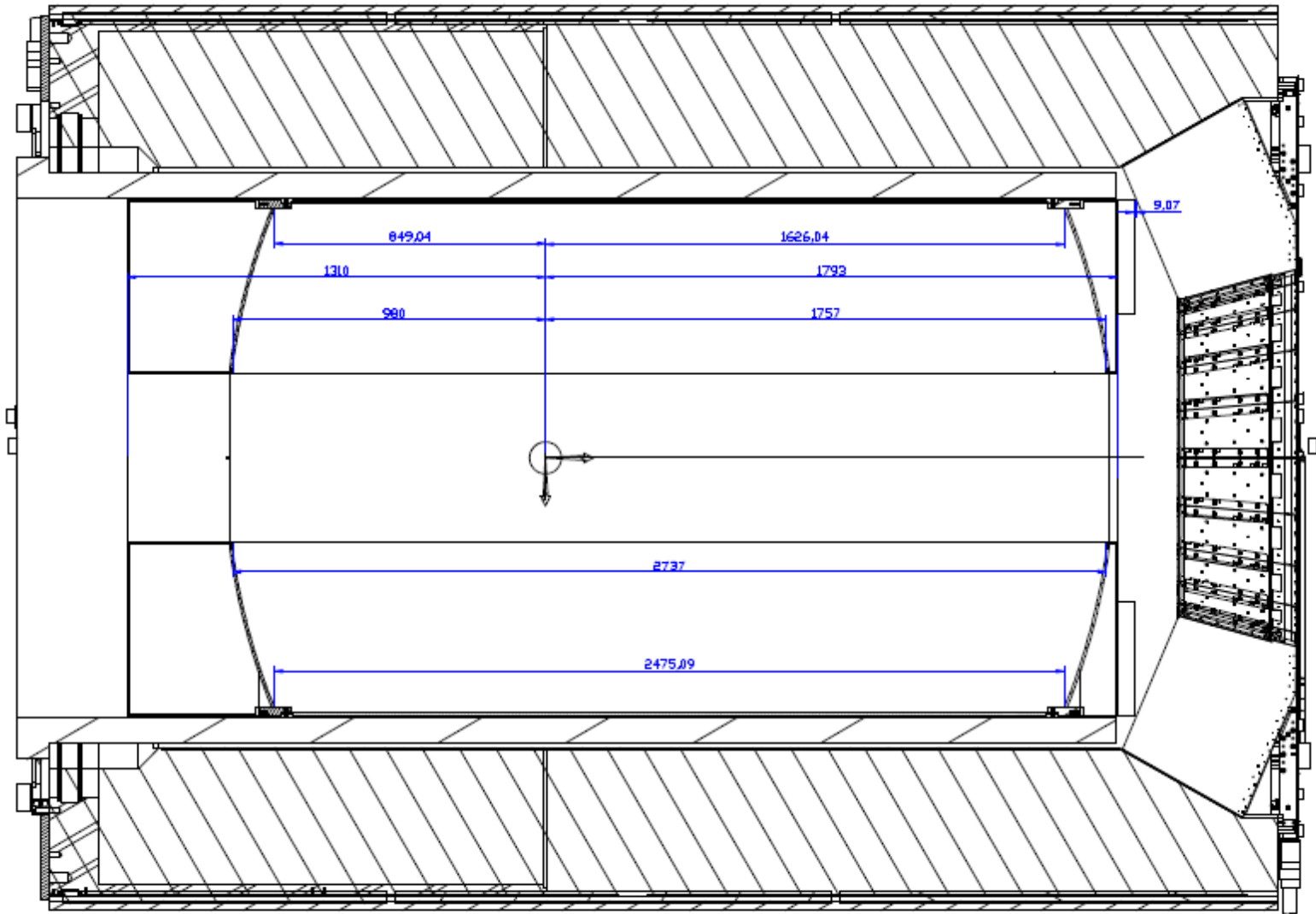
2) CONCAVE dimensions -1310 +1750



Drawing from Stefano Lauciani, LNF

210 mm

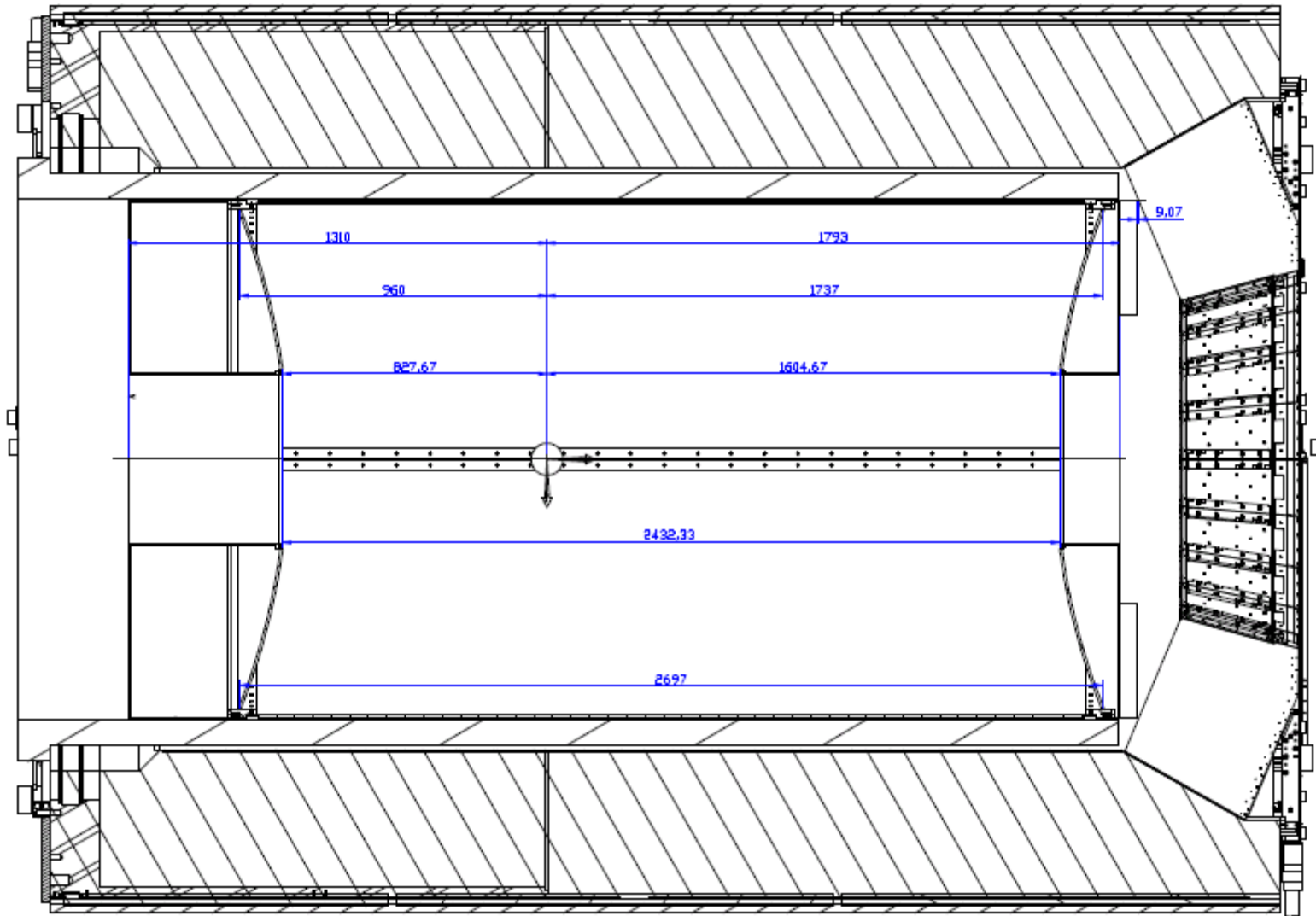
3) CONVEX dimensions -1310 +1793



210 mm

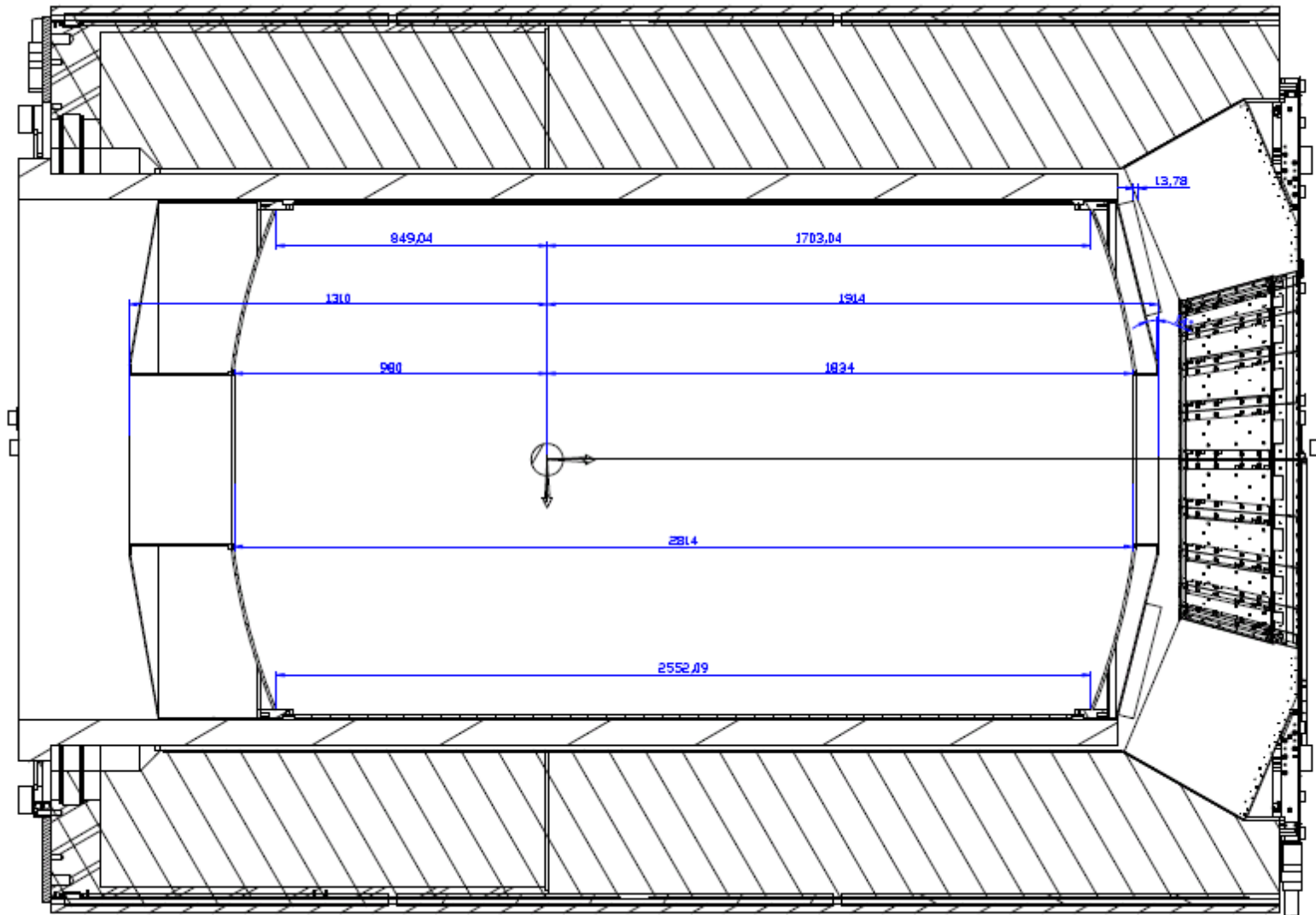
Drawing from Stefano Lauciani, LNF

4) CONCAVE dimensions -1310 +1793



Drawing from Stefano Lauciani, LNF

5) CONVEX dimensions -1310 +1914

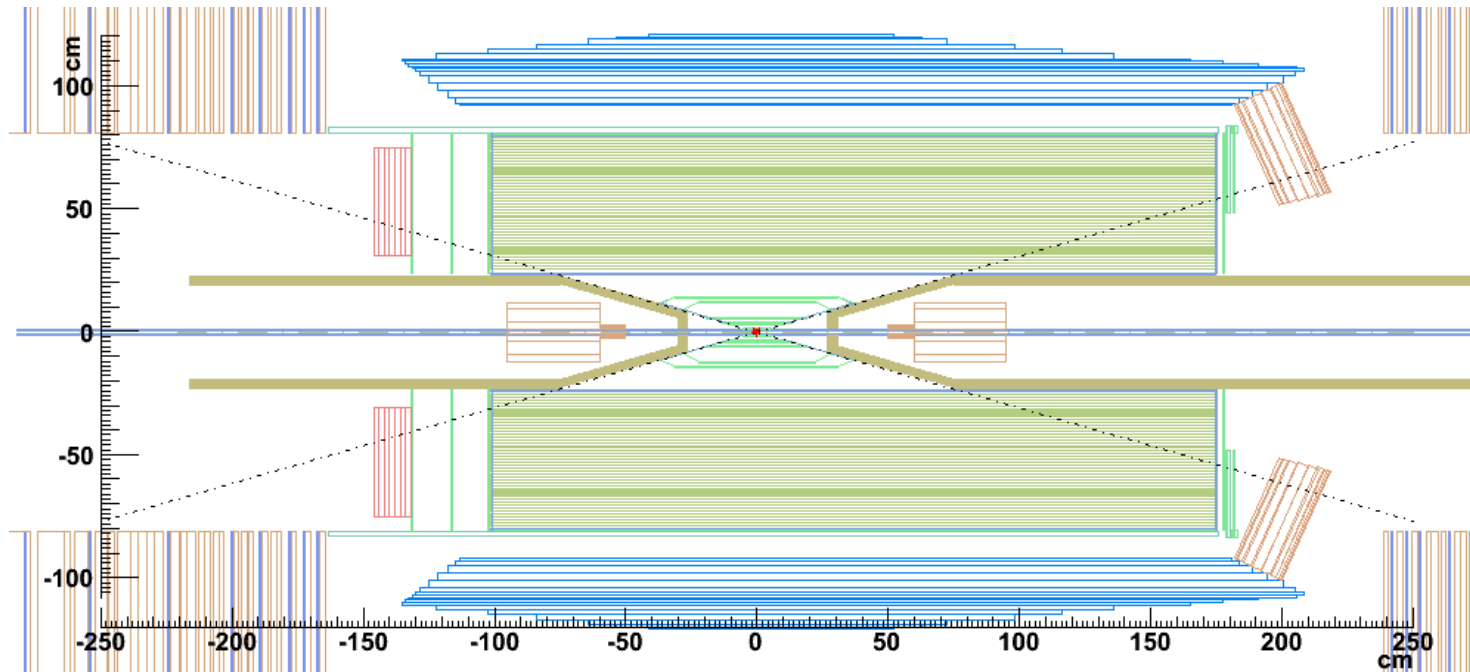


210 mm

Drawing from Stefano Lauciani, LNF

# Option 6

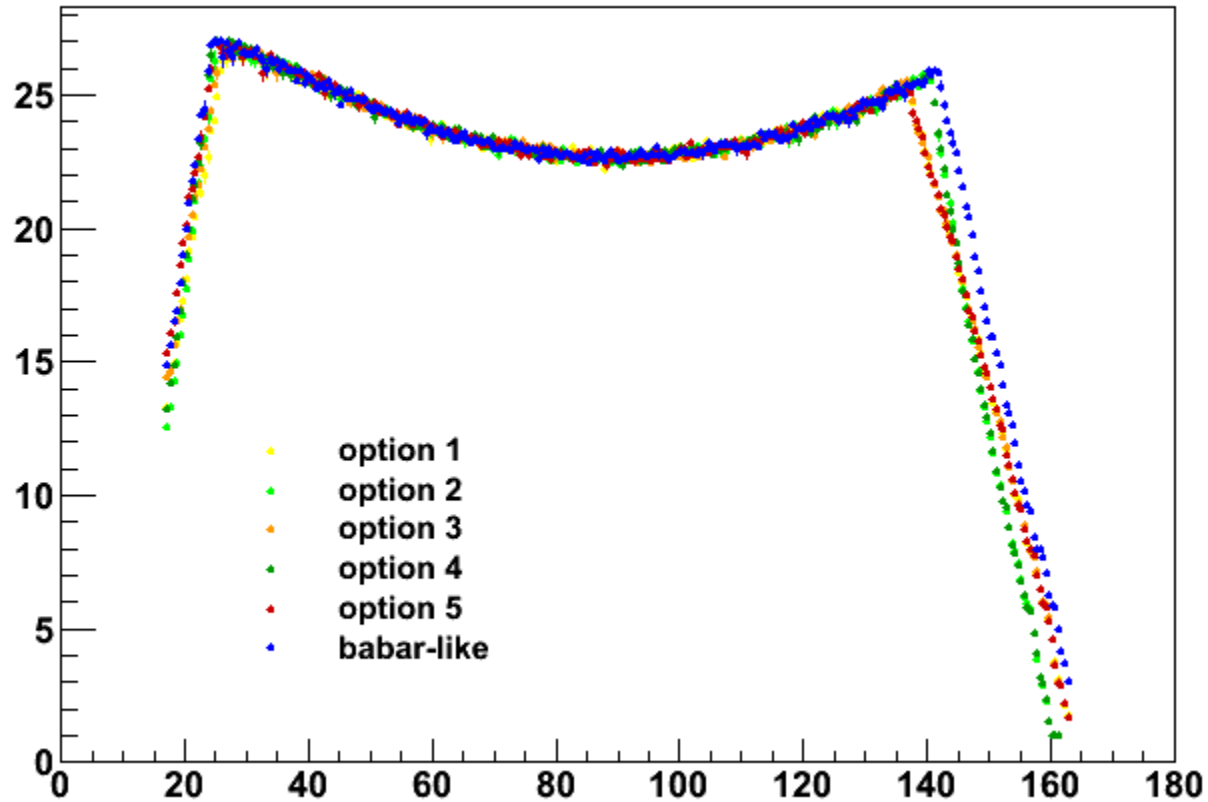
x-z layout in fastsim



old SuperB (babar-like) configuration

# single $\pi^+$ , $p=4\text{GeV}/c$ , flat $\cos\theta$

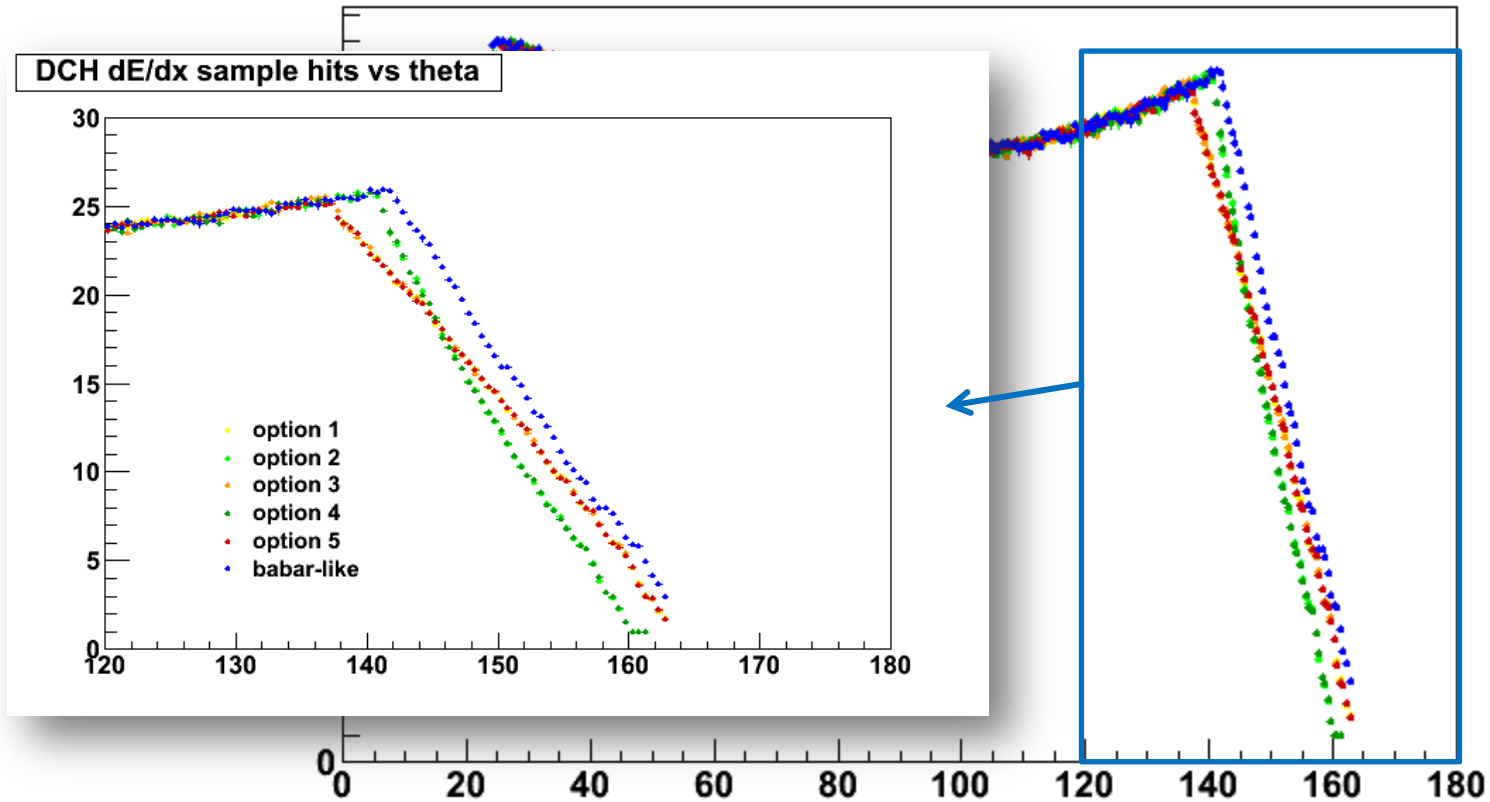
DCH dE/dx sample hits vs theta





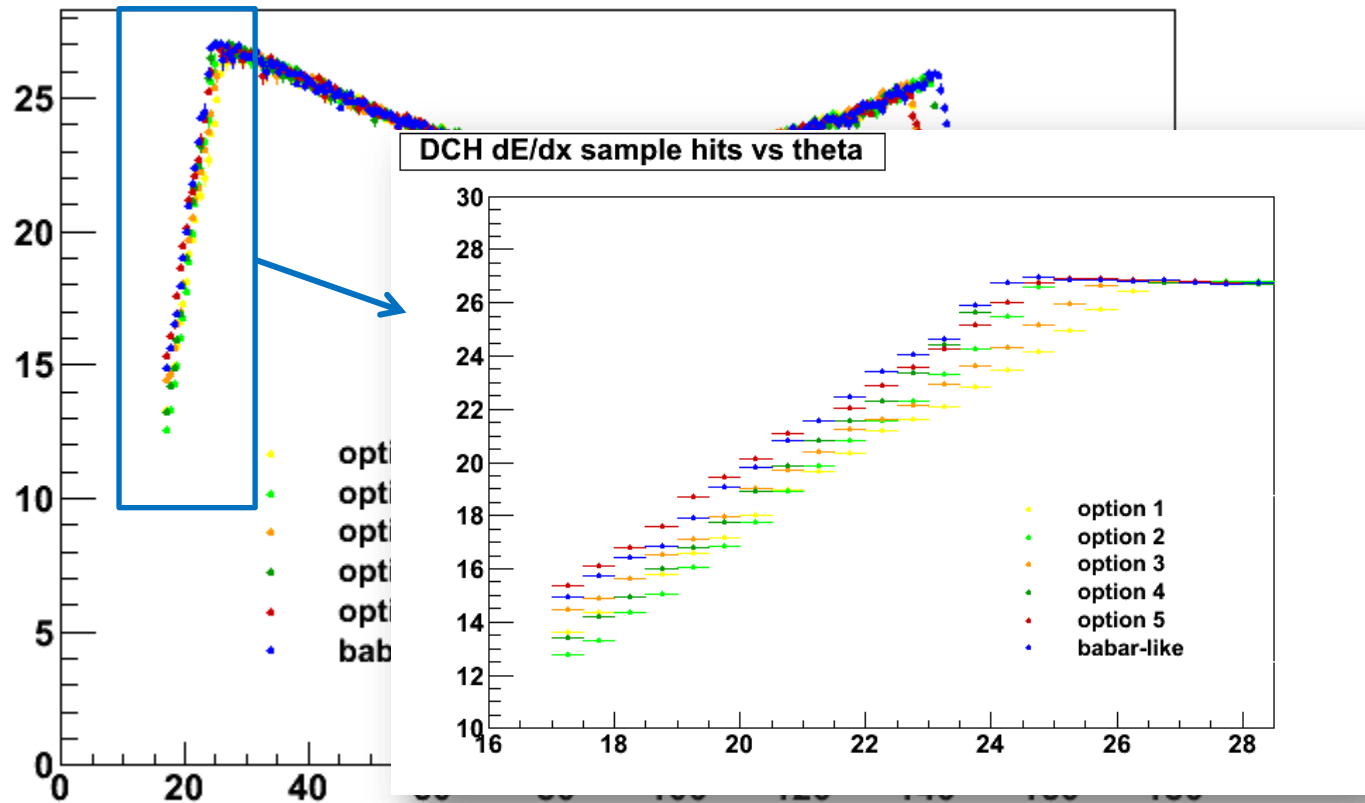
# single $\pi^+$ , $p=4\text{GeV}/c$ , flat $\cos\theta$

DCH dE/dx sample hits vs theta



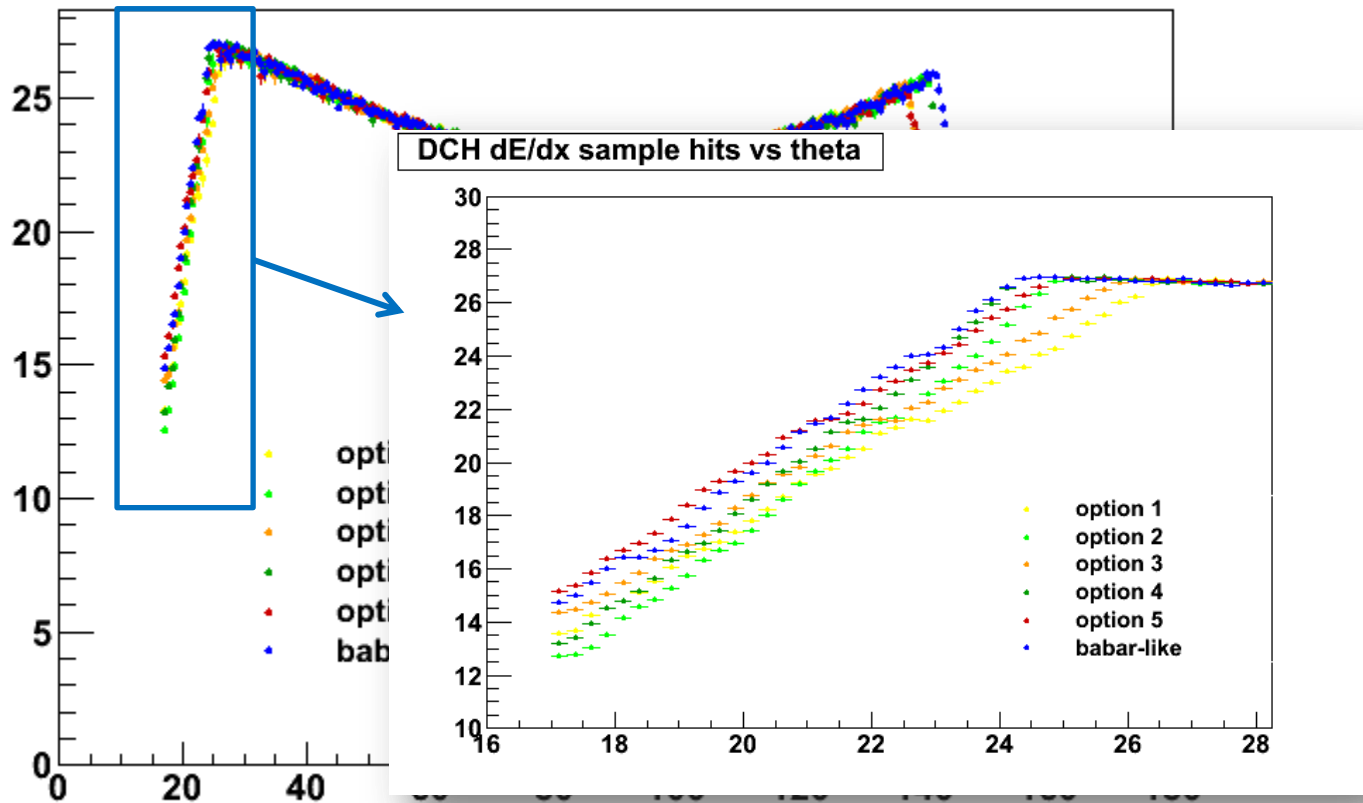
# single $\pi^+$ , $p=4\text{GeV}/c$ , flat $\cos\theta$

DCH dE/dx sample hits vs theta

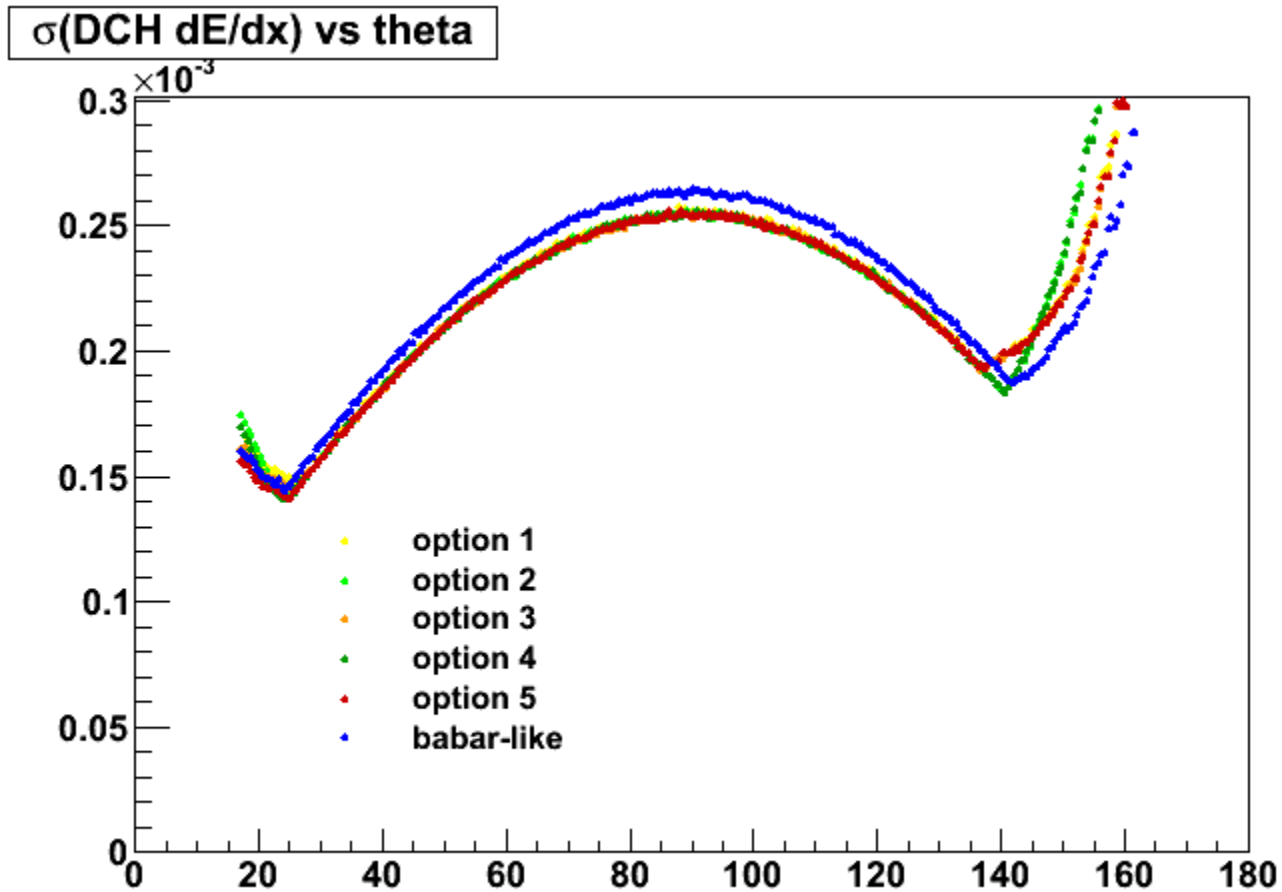


# single $\pi^+$ , $p=4\text{GeV}/c$ , flat $\cos\theta$

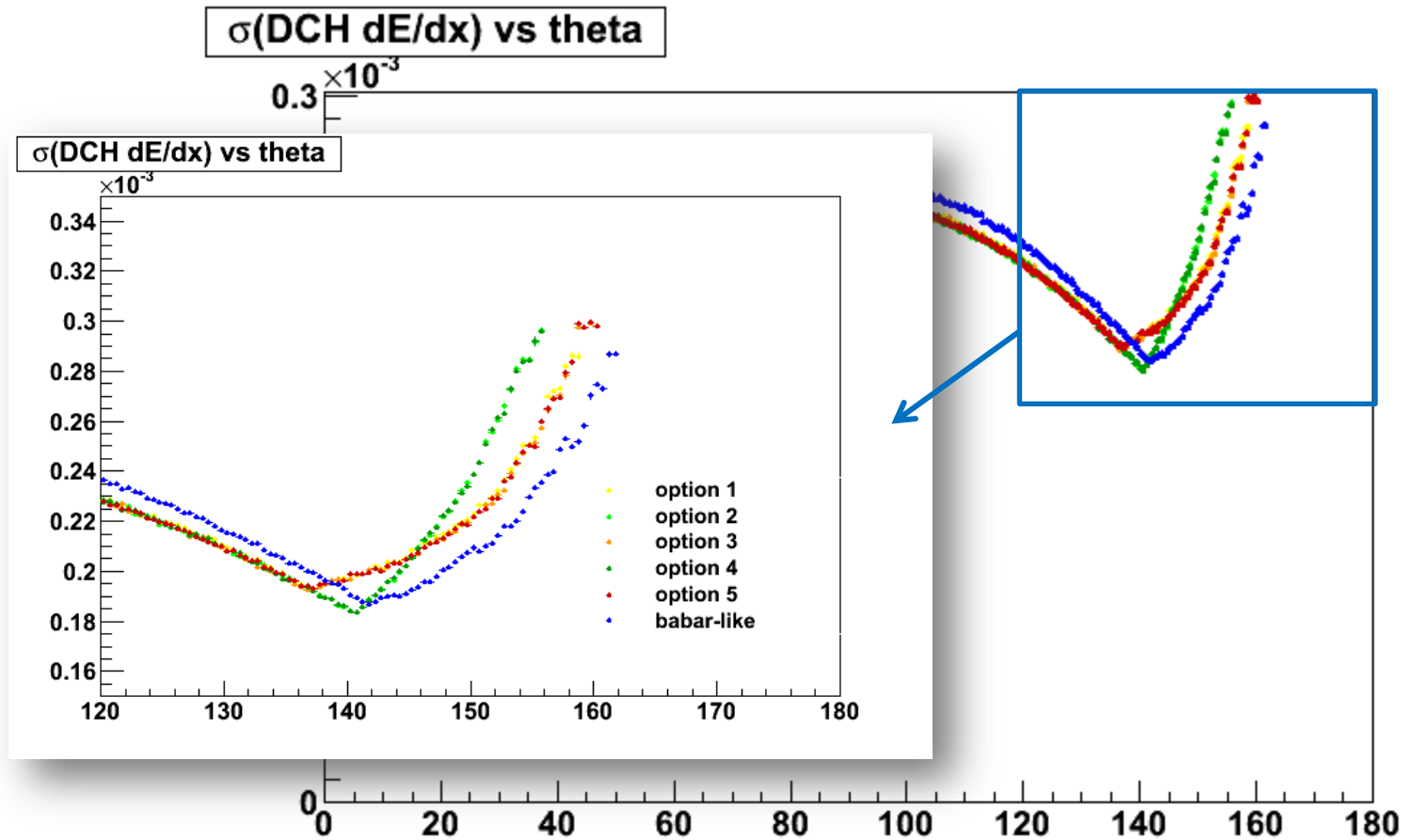
DCH dE/dx sample hits vs theta



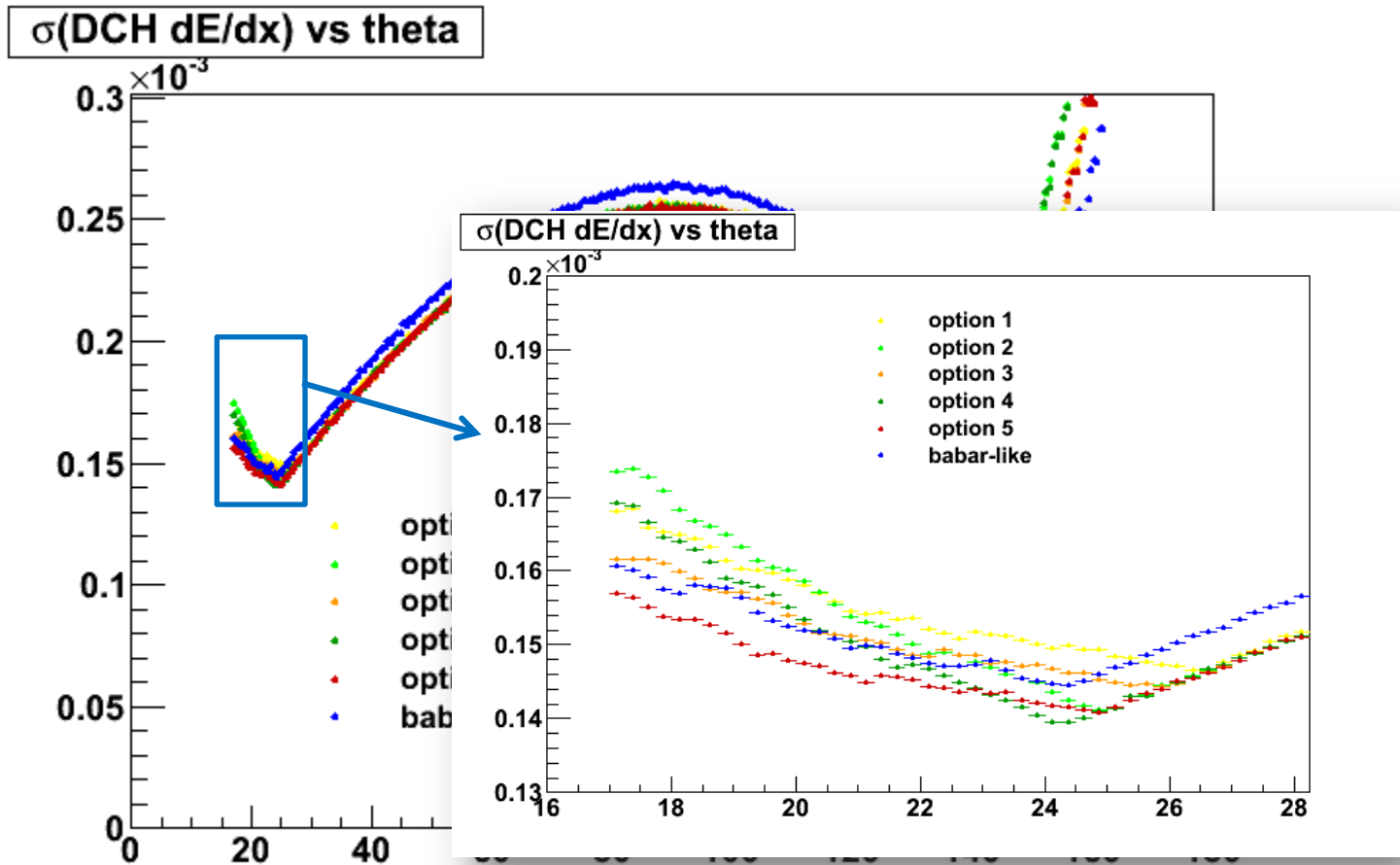
# single $\pi^+$ , $p=4\text{GeV}/c$ , flat $\cos\theta$



# single $\pi^+$ , $p=4\text{GeV}/c$ , flat $\cos\theta$

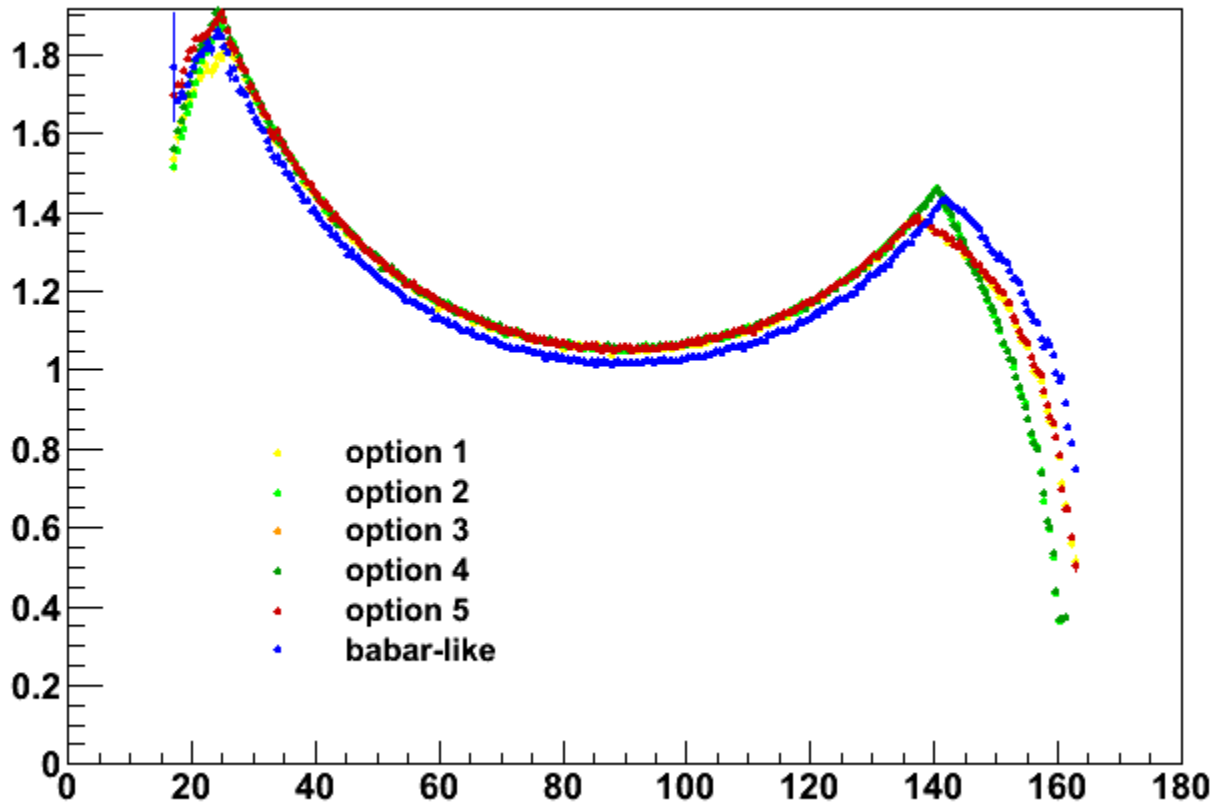


# single $\pi^+$ , $p=4\text{GeV}/c$ , flat $\cos\theta$



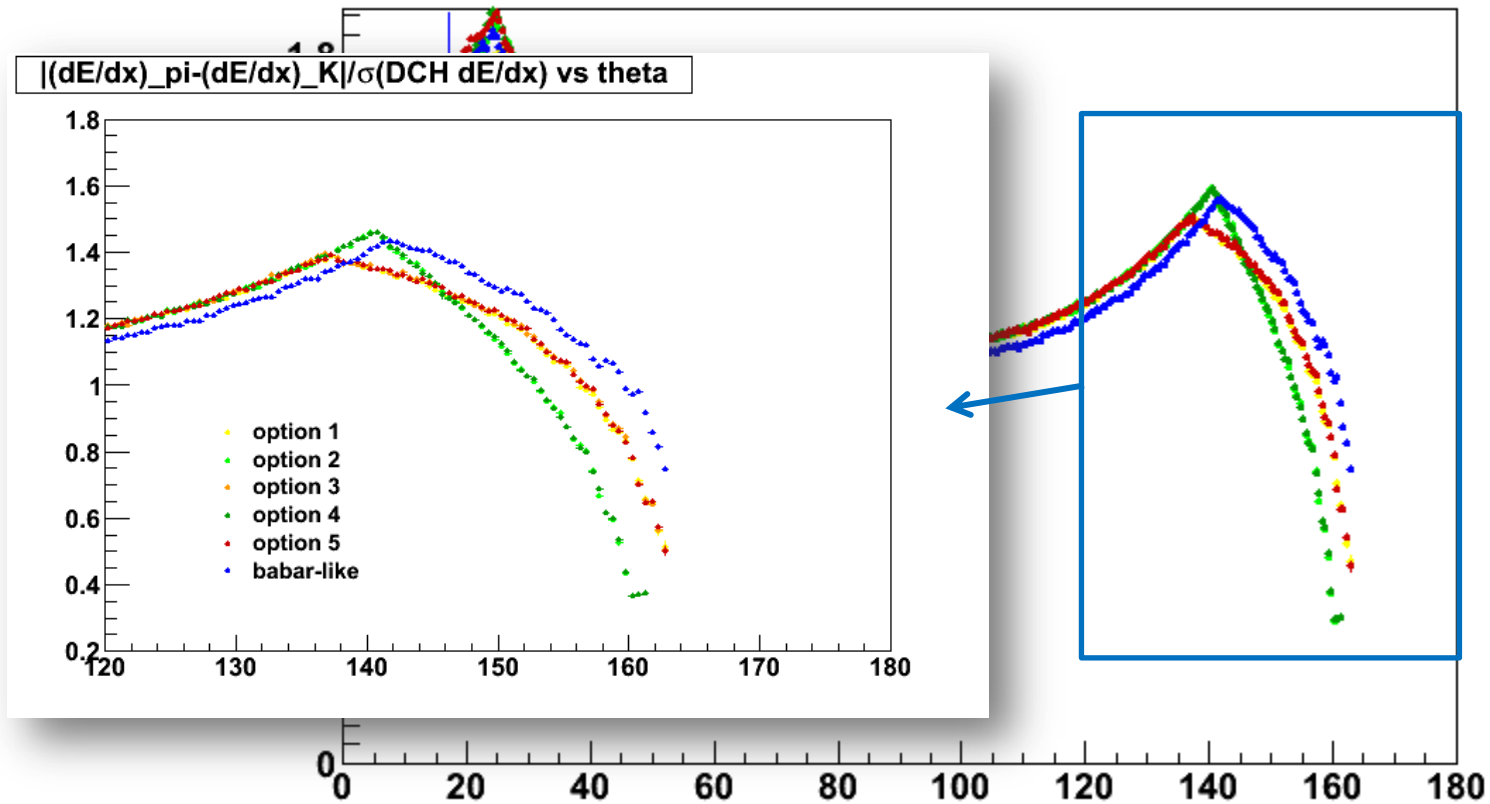
# single $\pi^+$ , $p=4\text{GeV}/c$ , flat $\cos\theta$

$|(dE/dx)_{\pi} - (dE/dx)_K| / \sigma(\text{DCH } dE/dx)$  vs theta



# single $\pi^+$ , $p=4\text{GeV}/c$ , flat $\cos\theta$

$|(\text{dE/dx})_{\pi} - (\text{dE/dx})_{\text{K}}| / \sigma(\text{DCH dE/dx})$  vs theta





# single $\pi^+$ , $p=4\text{GeV}/c$ , flat $\cos\theta$

$|(dE/dx)_{\pi} - (dE/dx)_K| / \sigma(\text{DCH } dE/dx)$  vs theta

